TRIBHUVAN UNIVERSITY

INSTITUTE OF ENGINEERING

PULCHOWK CAMPUS

THESIS NO:

A Study on Solar Air Heating System with Pebble Bed Energy Storage

by

Pradhumna Adhikari

A THESIS

SUBMITTED TO THE DEPARTMENT OF MECHANICAL ENGINEERING

IN PARTIAL FULFILLMENT OF THE REQUIREMENTS FOR THE

DEGREE OF MASTER OF SCIENCE IN RENEWABLE ENERGY

ENGINEERING

DEPARTMENT OF MECHANICAL ENGINEERING

LALITPUR, NEPAL

May 2016

COPYRIGHT

TRIBHUVAN UNIVERSITY

INSTITUTE OF ENGINEERING

PULCHOWK CAMPUS

DEPARTMENT OF MECHANICAL ENGINEERING

The undersigned certify that they have read, and recommended to the Institute of Engineering for acceptance, a thesis entitled **"A Study on Solar Air Heating System with Pebble Bed Energy Storage"** submitted by Pradhumna Adhikari, in partial fulfillment of the requirements for the degree of Master of Science in Renewable Energy Engineering.

_____

Supervisor, Prof. Rabindra Nath Bhattarai

Professor

Department of Mechanical Engineering

_____

External Examiner, Dr. Bivek Baral

Associate Professor

Kathmandu University

_____

Committee Chairperson, Dr. Rajendra Shrestha

Head

Department of Mechanical Engineering

Date: May 2016

ABSTRACT

A staggered type Solar Air Heater with aluminum absorber plate and selective coating was experimentally tested to know the performance parameters of the collector. It was found that the collector has maximum efficiency of around 65 % when operating at the air flowrate of 0.0645 kg/s while the efficiency reduced to around 34 % when the flow rate was reduced to 0.0344 kg/s.

The parameters obtained from the experimentation processes was utilized to integrate the collector and study the solar heating system for a general living dwelling of Kathmandu having floor area 150 sq. ft. The collector was integrated with pebble bed energy storage for heating during night time and off sunshine hours. Since the performance of collector is major factor for effective solar heating system, the product of collector heat removal factor and transmission absorption product $F_R(\tau\alpha)\ and$ collector heat removal factor and overall heat loss coefficient $F_R U_L$ values obtained from the experiments were utilized in the simulation to define the collector which therefore is the validated input for the major parameter of the simulation setup.

The model for the solar heating system was developed in the simulation software TRNSYS. The performance of system for heating months ranging from October to March were considered. When utilizing the 4 m^2 collector area and 0.0645 kg/s flow rate in the collector loop for the pebble bed of length 1.5 m and cross sectional area 0.81m^2, the solar fraction covered by pebble bed was found to be ranging from 0.14 for the Months of January to around 0.59 for October when the heating load was minimum.

ACKNOWLEDGEMENTS

I would like to express my gratitude towards my Project Supervisor Prof. Rabindra Nath Bhattarai for his constant supervision and guidance throughout the project duration.

I would like to acknowledge Er. Niraj Shrestha (CEO, Sun Works Nepal) for his genuine support throughout this project duration for providing help in experimentation process. I would also like to express my thanks to Er. Niranjan Bastakoti for his help and support throughout the research duration. I would also like to acknowledge Er. Bijay Raj Khanal for providing necessary measuring instruments for the experiment.

Lastly I express my sincere thanks to all who have supported and encouraged me for carrying out the research.

TABLE OF CONTENTS

LIST OF FIGURES

LIST OF TABLES

LIST OF SYMBOLS

h	Heat transfer coefficient [W/m^{2}K]
L	Plate spacing [m]
k	Thermal conductivity [W/m K]
g	Gravitational constant [m/s^2]
β'	Volumetric coefficient of expansion; for ideal gas, $\beta' = 1/T$.
v	Kinematic viscosity [m^2/s]
$\propto$	Thermal diffusivity [m^2/s]
β	collector tilt (deg)
ε_g, e_p	emittance of glass, plate
T_a	Ambient temperature (K)
T_{pm}	mean plate temperature (K)
h_w	wind heat transfer coefficeint (W/m^2°C)
F_R	Collector Heat Removal Factor
F'	Collector Efficiency Factor
F''	Collector Flow Factor
Pr	Prandtl Number
Nu	Nusselt Number
Re	Reyonld's Number

CHAPTER ONE

INTRODUCTION

1.1 Background

Solar energy systems can be classified as; solar thermal systems and solar PV systems. In solar thermal systems, the function of a solar collector is the conversion of solar radiation on its surface into energy (in the form of sensible or latent heat in a fluid, which is passed through the collecting unit). Numerous types of solar energy collectors have been devised in recent years among which Solar Air Heater (SAH) is commonly used device. (Saxena, et al., 2015)

Solar air heaters (SAHs) form the foremost component of solar energy utilization system. These air heaters absorb the irradiance and convert it into thermal energy at the absorbing surface and then transfer this energy to a fluid flowing through the collector. SAHs are inexpensive and most used collection devices because of their inherent simplicity. SAHs are found in several solar energy applications, especially for space heating, timber seasoning and agriculture drying and process heating applications. (Saxena, et al., 2015) SAHs are simple in design and require maintenance. Corrosion and leakage problems are less severe compared with the liquid heater solar systems. The main drawback of SAHs is that the heat-transfer coefficient between the absorber plate and the air stream is low, which results in a lower thermal efficiency of the heater. However, different modifications are suggested and applied to improve the heat-transfer coefficient between the absorber plate and air. (Ozgen, et al., 2009)

Solar energy is a time-dependent energy resource. Energy needs for a very wide variety of applications are also time dependent but in a different fashion than the solar energy supply. Consequently, the storage of energy or other product of a solar process is necessary if solar energy is to meet substantial portions of these energy needs. There are various forms of solar energy storage ranging from sensible to latent heat storage to chemical energy storage according to the need of the applications.

Energy storage systems are designed to accumulate energy when production exceeds demand and to make it available at the user's request. They can help match energy

supply and demand, exploit the variable production of renewable energy sources (e.g. solar and wind), increase the overall efficiency of the energy system.

In the typical temperate climatic conditions of Kathmandu Valley, space heating is required during months from October to March to fulfill which solar energy with thermal storage system can be effectively utilized to offset and supplement the heating requirements.

1.2 Problem Statement

Despite the simplicity, inexpensiveness and ease of maintenance application of Solar Air Heaters (SAHs) in several solar energy applications especially for space heating, timber seasoning and agriculture drying etc, there is research gap in the country regarding its study, development, utilization and efficiency improvements. A proper experimental testing, analysis and approaches to enhance the thermal efficiency of much utilized solar air collectors are lacking. Due to which, the intervention of SAH into various sectors are also nominal.

The utilization of SAHs in the space heating applications is very less practiced because of the lack of proper characterization and development of SAHs within country and due to the uneven nature of the Solar energy source which where the heating is mostly required in off sunshine hours during the heating season. So lack of proper development of integrated solar heating system with energy storage and auxiliary source.

Also no such study of the analysis of the heating system using the weather data of Kathmandu has been studied previously to study the response of the system during the whole heating period; the knowledge of which can further encourages to adopt the system into various application sectors.

1.3 Rationale

The most effective utilization of the SAHs are for agricultural crop drying and for space heating applications. Since Nepal being an agricultural country and various types of solar dryers being utilized in the process of agricultural crop drying, an effort to enhance the efficiency of the solar air heater from the conventional type seems logical. Also extensive use of such type of heating system could significantly decrease the utilization of biomass and fossil fuel used for space heating applications. The efficiency of the collectors plays a crucial role in the performance of the entire system

and from economical viewpoint. With increased efficiency, various economic benefits can be obtained. An application of efficient, economical and technologically furnished SAH in use can lead to the use of solar thermal energy in increased scale as well as it increase the productivity and effectiveness in the sector it is used. Also for space heating applications the utilization of energy is most required when the solar intensity is low and during off sunshine hours. So storage of energy in sensible heat in low cost materials like rocks, pebble beds etc. leads to the proper utilization of the solar energy.

1.4 Objectives

1.4.1 Main Objective

To study the Solar Air Heating System with pebble bed energy storage

1.4.2 Specific Objectives

- To experimentally determine the performance parameters of the staggered type Solar Air Heater
- To study the pebble bed energy storage as sensible heat storage medium to couple with the Solar Air Heater
- To simulate and study the performance of solar heating system and pebble bed storage in TRNSYS

1.5 Methodology

1.5.1 Methodological Tasks

A research methodology was followed to complete the specified objectives within the given frame of time. The methodology adapted was loosely based on experiences from similar researches conducted previously. A step by step methodology followed for the research is outlined as follows:

I. Problem Formulation

A research is aimed towards obtaining the solution of a problem. As such, the first step of the research was to formulate the problem and explore the potential solutions to resolving the formulated problem.

II. Literature Survey

Literature from various sources including journals, text books, and articles were extensively reviewed to obtain an in-depth understanding of the subject of research. Literatures focused on previous researches involving similar scope of study were prioritized and their findings and recommendations were analyzed.

III. Experimental Evaluation on the performance of the staggered type Solar Air Heater

The performance parameters of the staggered type solar air heater were conducted in the experimental setup. The parameters $F_R(\tau\alpha)\ and\ F_R U_L$ at two different flow rates thus obtained were utilized in the simulation environment; the performance of Solar Collector being crucial and most important component in the Solar Air Heating System

IV. Simulation Setup

To simulate the performance of the solar air collector in conjunction with the pebble bed energy storage for utilization of the energy for the heating purpose of simple living dwelling was considered. The simulation was carried out in TRNSYS simulation environment and the results were analyzed.

V. Analysis, Conclusion and Recommendation

The results from the simulation were analyzed in detail and conclusion and recommendations were drawn from the analysis of the results.

VI. Thesis Writing, Submission and Final Presentation

All the work done as the part of research was documented in the form of the report.

CHAPTER TWO

LITERATURE REVIEW

Solar energy collectors are special kinds of heat exchangers that transform solar radiation energy to internal energy of the transport medium. The major component of any solar system is the solar collector. This is a device that absorbs the incoming solar radiation, converts it into heat, and transfers the heat to a fluid (usually air, water, or oil) flowing through the collector. Solar collectors can also be distinguished by the type of heat transfer liquid used (water, non-freezing liquid, air, or heat transfer oil) and whether they are covered or uncovered. The three main types of stationary collectors are Flat Plate Collectors, Stationary compound parabolic collectors (CPCs), Evacuated tube collectors (ETCs). The advantages of flat-plate collectors are that they are inexpensive to manufacture, they collect both beam and diffuse radiation, and they are permanently fixed in position, so no tracking of the sun is required.

A simple flat plate SAH consists of one or more sheets of glass or transparent material situated above an absorbing plate with the ambient air flowing either over or under the absorbing, so it acts as a black body to absorb heat. The sun's rays pass through the glass and are trapped in the space between the covers and plate or absorbed into the black body. Except for the glass covers, all parts of a solar air heater are well insulated to make the energy loss as small as possible. The glass covers are employed to reduce convection and radiation losses into the atmosphere. (Ho, et al., 2011)

The main components of flat plate collectors are

- **Cover**: One or more sheets of glass or other radiation-transmitting material.
- **Heat removal fluid passageways**: Tubes, fins, or passages that conduct or direct the heat transfer fluid from the inlet to the outlet.
- **Absorber plate:** Flat, corrugated, or grooved plates, to which the tubes, fins, or passages are attached. The plate is usually coated with a high-absorptance, low-emittance layer.
- **Manifolds:** Pipes and ducts to admit and discharge the fluid.
- **Insulation**: Used to minimize the heat loss from the back and sides of the collector.

- **Container**: The casing surrounds the aforementioned components and protects them from dust, moisture, and any other material.

Flat-plate collectors have been built in a wide variety of designs and from many different materials. They have been used to heat fluids such as water, water plus antifreeze additive, or air. Their major purpose is to collect as much solar energy as possible at the lowest possible total cost. The collector should also have a long effective life, despite the adverse effects of the sun's ultraviolet radiation and corrosion and clogging because of acidity, alkalinity, or hardness of the heat transfer fluid, freezing of water, or deposition of dust or moisture on the glazing and breakage of the glazing from thermal expansion, hail, vandalism, or other causes. These causes can be minimized by the use of tempered glass. (Kalogirou, 2006)

2.1 Types of Solar Air Heater

SAH collects solar radiant energy and transforms it into heat through a fluid flowing inside the system. Basically, all SAHs can be classified under two categories

2.1.1 Air heaters with non-porous absorber plate

In this type, the air stream does not flow through the absorber tray. The air may flow above or beneath the absorber tray. The air that blows above the absorber surface increase the convection loss from the cover plate and therefore it is avoided, if the 'Ti' and size at the collector are large. Selective coating can be applied to improve collector efficiency. These can be classified as

1. Conventional air heater,
2. Air heaters with fins,
3. Vee-corrugated air heater
4. Double exposure heaters,
5. Double flow solar air heater
6. Two pass solar air heater.

2.1.2 Air heaters with porous absorber

A major disadvantage of the nonporous absorber is the necessity of capturing all incoming solar radiation over the projected area through a thin layer over the absorber's surface. If some selective coatings are used then radiative losses from the absorber can be minimized and unless the collection efficiency remains poor. The ΔP

along the duct formed between the absorber plate and the rear insulation may also be prohibitive, especially in the case of added fins to increase the heat transfer area and turbulence rate. The porous absorber SAHs can be classified as given below

1. Packed bed solar air heater,
2. Overlapped glass plate air heater,
3. Matrix air heater,
4. Honeycomb porous bed air heater and
5. All plastic solar air heaters.

2.2 Construction of Solar Air heater

There are various types of SAHs and the key components (as discussed in Section 1.3) of these systems are; a blackened absorber (normally made from a thin Aluminum sheet), a thin transparent glass (glazing), the ducts, an air blower or fans and insulation material. In brief, a transparent glass is used to allow solar radiation inside the SAH and an Al or G.I. (sometimes, tin is also used) blackened thin sheet is used to store the solar energy in a good amount.

2.2.1 Ducts

In SAHs, the ducts are used to supply the fresh air and exhaust of warm/hot air by the means of natural and forced convection. It is notable that the air velocity is a majorly considerable factor in efficiency effecting parameters of a SAH. It has also been noticed that the artificial surface roughness provided on the ducts or on the absorber plates of SAHs has a favorable effect on the heat transfer. Because the artificial geometry creates turbulence in laminar sub-layer due to flow separation and reattachment between the two repeated ribs therefore the ‘h’ increases between the absorber plate and the flowing fluid in a SAH. Recirculation flow further enhances the convective heat transfer. It was found that perforation in ribs/baffles/ blocks and combination of these, leads to heat transfer augmentation and the better thermo-hydraulic performance.

In an approach to increase the thermal efficiency of SAHs, various researchers have employed various techniques with promising results. Ming Yang et al (Wang, 2014) designed and optimized SAH with offset strip fin absorber plate. Reheleh et al (Nowzari, et al., 2015) studied the best configuration for a solar air heater by design and analysis of experiment and concluded that double-pass solar collector with a

quarter- perforated cover with 3-cm hole-to-hole spacing and mass flow rate of 0.032 kg/s yielded best results. Romdhane, 2007 comparatively studied the introduction of baffles in SAH to favor the heat transfer

2.2.2 Glazing

A glazing (a transparent glass) plays a vital role to allow the incident solar radiation for entering the device and substantially restricting infrared energy losses through re-radiation. A glazing should be used for a high transmissivity to the solar spectrum and extensively opaque to long (or infrared) wavelength solar radiation One or more sheets of transparent glass are used to transfer the energy from the sun into the solar collector or absorber inside the solar system. The transparent glazing is purposely used to reduce convection losses from the absorber to the environment through the restraint of the stagnant fluid layer in between the absorber and glazing. Glazing also reduces radiation losses from the solar collector (because of a transparent glass) to the short wave radiation received from the sun, but it is almost opaque to long-wave thermal radiation emitted by the absorber. Glazing materials include glass, plastics, acrylics, fiberglass and other transparent materials.

2.2.3 Absorber tray

An absorber tray/plate is the main component of a SAH and has a momentous effect on thermal performance of a solar thermal system. Many aspects of materials (mainly absorptivity of solar heat) and their properties have a significant effect on the overall performance and the cost of a solar energy device. The major concern will be with different materials as applied to solar collectors, with a reflection to material properties as they affect the overall performance. Basic studies for absorptivity reasons have suggested numerous mechanisms for a selection of energy- absorbing surfaces. These mechanisms, include:(i) variant optical constants index (refractive and absorptive) with wavelength (λ) for a particular surface material; (ii) dimensions of the surface roughness of large comparative to an extent value of ‘λ’, but slightly depend on long-wave re-radiation; (iii) coatings of small particles of measurements larger than ‘λ’ but lesser than long- wave re-radiation;(iv) thin anti-reflection coating for increasing absorptivity; and (v) and thick semiconductor films. Although, selective surfaces has a significant effect on the performance of SAHs, but SAHs carrying a

blackened absorber plate are still exclusively used because of difficulty of producing selective surfaces by the inexperienced.

2.2.4 Insulation

Thermal insulation is the simplest way to prevent heat losses and to achieve economy in energy usage especially in solar thermal systems. Thermal insulation serves many significant functions such as, to conserve energy, to reduce heat loss or heat gain, to maintain an efficient operation of the system (or chemical reaction), to assist in sustaining a product at a constant temperature, to prevent condensation, to create a comfortable environmental, to protect personnel and for Thermal Energy Storage (TES). Conventional insulation materials are often opaque and suitably classified into, fibrous, cellular, granular and reflecting type materials. Some commonly used thermal insulation materials areas; glass, fiber, alumina silicate, mineral wool and calcium silicate, among which the glass-wool has been noticed to be used as an insulation SAHS, commonly. There are some definite losses from a thermal energy system, insulated with opaque type materials.

2.3 Various Models of Solar Air Heater

It has been observed that a solar thermal system can enhance the performance by using SAHs with, a TES material, a CPC or PTC, and hybrid systems. Where, one side a TES material (in the form of SHS or LHS) improve the performance the system in the off sunshine hours, thereon, a CPC or PTC increased the efficiency during the sun shine hours by focusing the solar irradiance on the system. Apart this, hybrid systems (SAHs) can be operated on an alternative fuel besides solar energy such as; electrical back up or fossil fuel. In the upcoming sub- sections a detailed study of these systems has been presented.

2.3.1 Solar Air Heater with Thermal Storages

Storage of solar energy is an imperative for future success of solar energy employment. The main problem is assortment of materials having appropriate thermo-physical characteristics in which solar energy can best stored in the form of heat. These materials can divide into two broad categories; those that store energy in the form of sensible heat; and those that undergo a change of state or physical– chemical change at a certain temperature within the practical range of temperature provided by

the solar heat collectors. The thermal heat storages purposely for use solar thermal applications are;

(i) Sensible heat storage (SHS): as sensible heat in solids (rocks or water). The heat storage medium, thereby experiences an increase in temperature without undergoing a change in its phase,

(ii) Latent heat storage (LHS): as latent heat of fusion in suitable chemical compounds (paraffin waxes and in organic salts). By using these heat storing materials one cannot only improve the thermal performance of a SAH but extend the duration of heating up to long hours. Besides this, good heat storing capacities of these materials are very useful for solar thermal systems to perform in poor ambient conditions or in the night.

In an extensive review conducted by Saxena & Goel, 2013 on Solar Air Heaters with Thermal Heat Storages they found that TES has a significant effect on the thermal performance of SAHs. They concluded that rock bed, brick, concrete, water or iron gravels are low rating TES materials for solar applications because of low heat capacity and PCMs like paraffin wax and Glauber's slat fare useful because of having good capacity to store a comparatively large amount of heat.

The thermal analysis and exergy evaluation of packed bed storage system carried out by Bindra, et al., 2013 concluded that for packed beds, sensible heat storage system can provide much higher exergy recovery as compared to phase change material storage system under similar high temperature storage conditions.

In a review conducted on packed bed solar energy storage systems by Singh, et al., 2010 they reviewed various performance analysis of the packed bed system which was reported in the literature which included design of packed bed, materials used for storage, heat transfer enhancements, flow phenomenon and pressure drop through packed beds. And they also concluded that most of the studies carried out are on rocks and pebbles as packing materials.

Singh, et al., 2015 studied Thermal performance of packed bed heat storage system for solar air heaters under varying solar and ambient conditions in different months. The insulated packed bed heat storage unit was filled with 8500 kg rock pebbles. The solar collection and heat retrieval efficiency of 36– heat storage system ranged between 51% and 75–77%, respectively. Heat retrieval efficiency of the developed

packed bed was found better as compared to the packed bed filled with phase change material (PCM)

In another study of solar air heating system conducted by Zhao, et al., 2011 on a solar heating system with pebble bed energy stoage was modeled through TRNSYS for a 3319 m^2 building and system optimisation was carried out by varying solar collector area, installation angle of solar collector, mass flow rate through the system, volume of pebble bed, heat transfer coefficient of insulation layer of pebble bed etc and the results showed that the designed solar system can meet 32.8 % of the thermal energy demand in the heating season and 84.6 % of the energy consumption in non-heating season, with a yearly average solar fraction of 53.04%.

Similarly, an optimization study carried out by Choudhury, et al., 1995 on design and operational parametrs of a rock bed thermal energy storage device coupled to a two pass single cover solar air heater that included charging time, rock bed size. Cross sectional area per square cross section, rock size, air mass velocity and void fraction.

Melo & Persson, 2013 carried out a research on Economic Evaluation of Solar Charge Enegy Storage for Space Heating on a building model of 2700 m^3 on TRNSYS and carried out economic optimization.

Raghav & Nagpal, 2015 carried out optimization of low temperature sensible heat solar energy storage system to investigate the behaviour of rock bed solar energy storage system. The overall performance of such system is influenced signifcantly by temperature distribution in storage unit which is affected by the system parameters; void fraction and equivalent diameter. They evaluate the peformance based on temeprature distribution, thermal energy stored, volumetric heat transfer coefficient, pressure drop characteristics and availabe energy stored in the bed.

A performance comparision between air and liquid residential solar heating system was carried out by Karaki, et al., 1978 on similar houses with flat plate liquid heating system in one house and flat plate air heating system in another house. Approximately 40 percent more energy was collected during the heating season with the air heating system because the air system opearted over a longer period of time.

Following the literature review, an experimental study of Solar Air Heater Coupled with Thermal Energy Storage for the reliability of the system is felt in context of extensive scope and possibility of utilization of Solar Air Heater in context of Nepal.

CHAPTER THREE

PARAMETERS OF THE SOLAR AIR COLLECTOR

3.1 Basic Equations for Flat Plate Collectors

The basic parameter to consider is the collector thermal efficiency. This is defined as the ratio of the useful energy delivered to the energy incident on the collector aperture. The incident solar flux consists of direct and diffuse radiation. While flat-plate collectors can collect both, concentrating collectors can utilize direct radiation only if the concentration ratio is greater than 10. (Duffie & Beckman, 2013)

3.1.1 Radiation Exchange for flat Plate Collectors

The majority of heat transfer problems in solar energy applications involve radiation between two surfaces

$$Q_1 = -Q_2 = \frac{\sigma(T_2^4 - T_1^4)}{\frac{1-\epsilon_1}{\varepsilon_1 A_1} + \frac{1}{A_1 F_{12}} + \frac{1-\epsilon_2}{\varepsilon A_2}}$$

For radiation between two infinite parallel plates (i.e., as in flat-plate collectors) the areas A_1 and A_2 are equal and the view factor F_{12} is unity. Under these conditions above Equation becomes

$$\frac{Q}{A} = \frac{\sigma\left(T_2^4 - T_1^4\right)}{\frac{1}{\varepsilon_1} + \frac{1}{\varepsilon_2} - 1}$$ (Duffie & Beckman, 2013)

3.1.2 Natural Convection between Flat Parallel Plates

The rate of heat transfer between two plates inclined at some angle to the horizon is of obvious importance in the performance of flat-plate collectors. Free-convection heat transfer data are usually correlated in terms of two or three dimensionless parameters: the Nusselt number Nu, the Rayleigh number Ra, and the Prandtl number Pr. Some authors correlate data in terms of the Grashof number, which is the ratio of the Rayleigh number to the Prandtl number.

The Nusselt, Rayleigh, and Prandtl numbers are given by

$$Nu = \frac{hL}{k}$$

$$Ra = \frac{g\beta' \Delta T L^3}{v \propto}$$

$$Pr = \frac{v}{\propto}$$ (Duffie & Beckman, 2013)

Where,

h =Heat transfer coefficient [W/m^{2}K]

L = Plate spacing [m]

k = Thermal conductivity [W/m K]

g = Gravitational constant [m/s^2]

β' = Volumetric coefficient of expansion; for ideal gas, β' =1/T.

ΔT = Temperature difference between plates [K]

v = Kinematic viscosity [m^2/s]

$\propto$= Thermal diffusivity [m^2/s]

For parallel plates the Nusselt number is the ratio of a pure conduction resistance to a convection resistance [i.e., Nu = (L/k) / (1/h)] so that a Nusselt number of unity represents pure conduction

Hollands et al. (1976) give the relationship between the Nusselt number and Rayleigh number for tilt angles from 0 to 75^0 as

$Nu = 1 + 1.446\left[1 - \frac{1708}{Ra \times \cos(\theta)}\right]^{+}\left\{1 - \frac{1708[\sin(1.8\theta)]^{1.6}}{Ra \times \cos(\theta)}\right\} + \left\{\left[Ra \times \frac{\cos(\theta)}{5830}\right]^{0.333} - 1\right\}^{+}$ (Duffie & Beckman, 2013) where the plus sign represents positive values only.

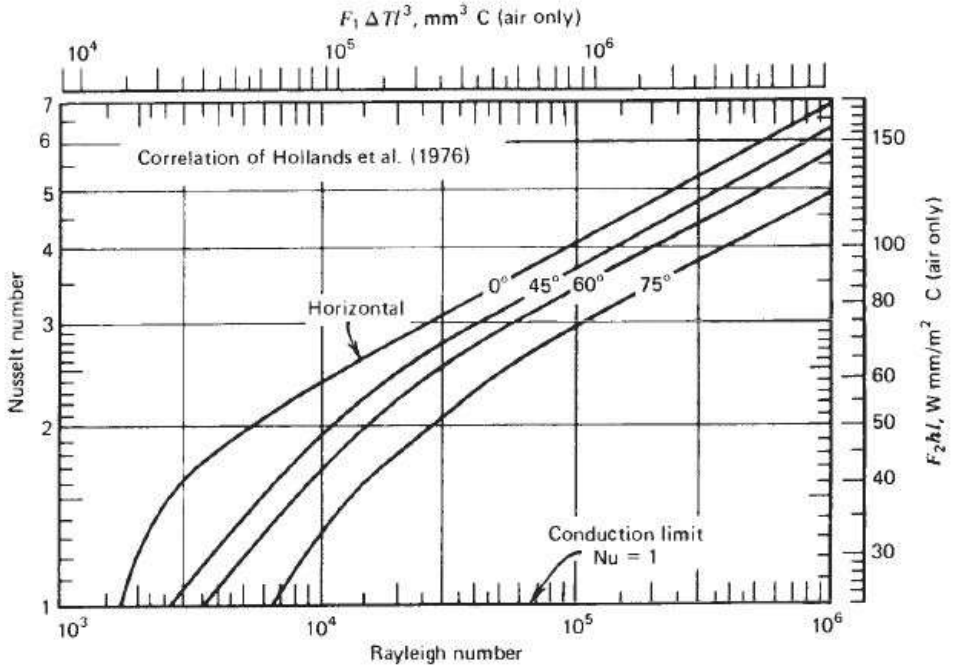

Figure 3.1 Nusselt number as a function of Rayleigh number for free-convection heat transfer (Duffie & Beckman, 2013)

3.1.3 Wind Convection Coefficient

The heat loss from flat plates exposed to outside winds is important in the study of solar collectors. Sparrow et al. did wind tunnel studies on rectangular plates at various orientations and found the following correlation over the Reynolds number range of 2×10^4 to 9×10^4

$Nu = 0.86\, Re^{\frac{1}{2}} Pr^{\frac{1}{3}}$ (Duffie & Beckman, 2013)

3.1.4 Transmittance-Absorptance Product

It is necessary to evaluate the transmittance absorptance product (τα). Of the radiation passing through the cover system and incident on the plate, some is reflected back to the cover system. However, all this radiation is not lost since some of it is, in turn, reflected back to the plate

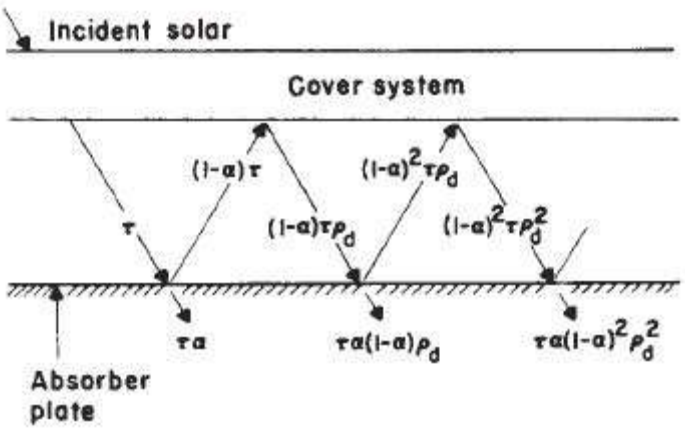

Figure 3.2 Absorption of solar radiation by absorber plate under a cover system. (Duffie & Beckman, 2013)

The situation is illustrated in Figure 3.2, where τ is the transmittance of the cover system at the desired angle and α is the angular absorptance of the absorber plate. Of the incident energy, $\tau\alpha$ is absorbed by the absorber plate and $(1 - \alpha)\,\tau$ is reflected back to the cover system. The reflection from the absorber plate is assumed to be diffuse (and unpolarized) so the fraction $(1 - \alpha)\,\tau$ that strikes the cover system is diffuse radiation and $(1 - \alpha)\,\tau\rho_d$ is reflected back to the absorber plate. The quantity ρ_d refers to the reflectance of the cover system for diffuse radiation incident from the bottom side

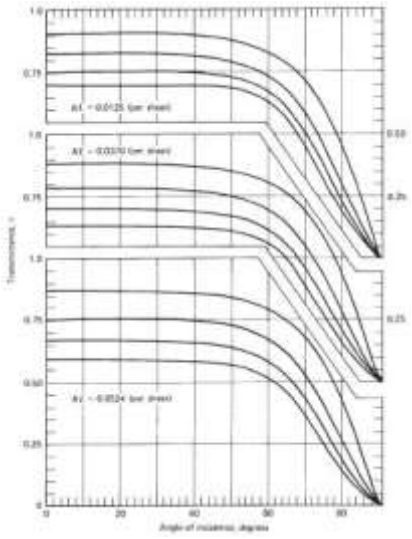

Figure 3.3 Transmittance (considering absorption and reflection) of one, two, three, and four covers for three types of glass (Duffie & Beckman, 2013)

3.1.5 Basic Energy Balance Equation

In steady state, the performance of a solar collector is described by an energy balance that indicates the distribution of incident solar energy into useful energy gain, thermal losses, and optical losses. The solar radiation absorbed by a collector per unit area of absorber S is equal to the difference between the incident solar radiation and the optical losses. The thermal energy lost from the collector to the surroundings by conduction, convection, and infrared radiation can be represented as the product of a heat transfer coefficient U_L times the difference between the mean absorber plate temperature T_{pm} and the ambient temperature Ta. In steady state the useful energy output of a collector of area Ac is the difference between the absorbed solar radiation and the thermal loss

$$Q_u = A_C[S - U_L(T_{pm} - T_a)] \qquad \text{(ASHRAE, 2008)}$$

The problem with this equation is that the mean absorber plate temperature is difficult to calculate or measure since it is a function of the collector design, the incident solar radiation, and the entering fluid conditions

If conditions are constant over a time period, the efficiency is given by

$$\eta = Q_u / I_t A_c$$

The design of a solar energy system is concerned with obtaining minimum-cost energy.

Thus, it may be desirable to design a collector with efficiency lower than is technologically possible if the cost is significantly reduced. In any event, it is necessary to be able to predict the performance of a collector

3.1.6 Collector Overall Heat Loss Coefficient

When a certain amount of solar radiation falls on the surface of a collector, most of it is absorbed and delivered to the transport fluid, and it is carried away as useful energy. However, as in all thermal systems, heat losses to the environment by various modes of heat transfer are inevitable. The thermal network for a single-cover, flat-plate collector in terms of conduction, convection, and radiation is shown in Figure 3.4 and in terms of the resistance between plates in Figure 3.4 b . The temperature of the plate is T_p, the collector back temperature is T_b, and the absorbed solar radiation is S. The energy losses from the collector can be written as

$$Q_{loss} = \frac{T_p - T_a}{R_L} = U_L A_c (T_p - T_a)$$

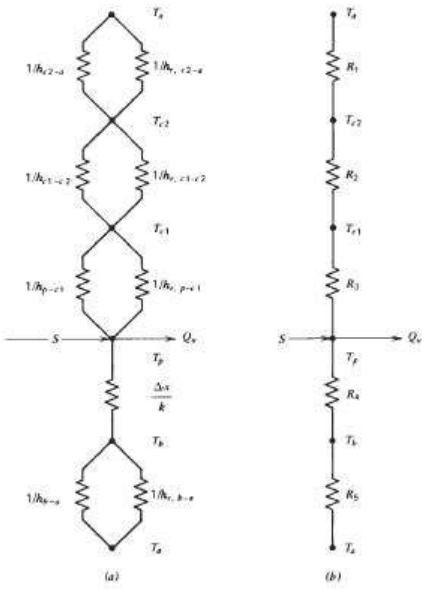

Figure 3.4 Thermal network for a two-cover flat-plate collector: (a) in terms of conduction, convection, and radiation resistances; (b) in terms of resistances between plates. (Duffie & Beckman, 2013)

For this two-cover system, the top loss coefficient from the collector plate to the ambient is

$$U_t = \frac{1}{R_1 + R_2 + R_3}$$

An empirical equation for U_t was developed by Klein (1979) following the basic procedure of Hottel and Woertz (1942) and Klein (1975).

$$U_t = \left(\frac{N}{\frac{C}{T_{pm}} \left[\frac{(T_{pm} - T_a)}{(N+f)} \right]^e} + \frac{1}{h_w} \right)^{-1} + \frac{\sigma (T_{pm} + T_a)(T_{pm}^2 + T_a^2)}{\frac{1}{\varepsilon_p + 0.00591 N h_w} + \frac{2N + f - 1 + 0.133\varepsilon_p}{\varepsilon_g} - N}$$

(Duffie & Beckman, 2013) Where

N = number of glass covers

$f = \left(1 + 0.089 h_w - 0.1166 h_w \varepsilon_p\right)(1 + 0.07866 N)$

$C = 520(1 - 0.000051\beta^2)$ for $0° < \beta < 70°$;

$e = 0.430(1 - 100/T_{pm})$

β = collector tilt (deg)

ε_g, e_p = emittance of glass, plate

T_a = Ambient temperature (K)

T_{pm} = mean plate temperature (K)

h_w = wind heat transfer coefficeint ($W/m^2°C$)

The magnitudes of R_4 and R_5 are such that it is usually possible to assume R_5 is zero and all resistance to heat flow is due to the insulation. Thus, the back loss coefficient U_b is approximately

$$U_b = \frac{1}{R_4} = \frac{k}{L}$$

where k and L are the insulation thermal conductivity and thickness, respectively.

Tabor (1958) recommends edge insulation of about the same thickness as bottom insulation. The edge losses are then estimated by assuming one-dimensional sideways heat flow around the perimeter of the collector system. The losses through the edge should be referenced to the collector area. If the edge loss coefficient–area product is (U/A) edge, then the edge loss coefficient, based on the collector area Ac, is

$$U_e = \frac{(UA)_{edge}}{A_C}$$

3.1.7 Collector Efficiency Factor

Collector Efficiency Factor (F′) represents the ratio of the actual useful energy gain to the useful gain that would result if the collector absorbing surface had been at the local fluid temperature. F′is the ratio between, $F' = U_o/U_L$

The collector efficiency factor is essentially a constant for any collector design and fluid flow rate.

3.1.8 Collector Heat Removal Factor and Flow Factor

It is convenient to define a quantity that relates the actual useful energy gain of a collector to the useful gain if the whole collector surface were at the fluid inlet temperature. This quantity is called the collector heat removal factor FR. In equation form it is

$$F_R = \frac{\dot{m}C_p(T_{fo} - T_{fi})}{A_c[S - U_L(T_{fi} - T_a)]}$$

The collector heat removal factor can be expressed as

$$F_R = \frac{\dot{m}C_P}{A_c U_L}\left[1 - \exp\left(-\frac{A_c U_L F'}{\dot{m}C_P}\right)\right]$$

To present above equation graphically, it is convenient to define the collector flow factor F'' as a ratio of F_R to F'. Thus

$F'' = \frac{F_R}{F'} = \frac{\dot{m}C_P}{A_c U_L F'}\left[1 - exp\left(-\frac{A_c U_L F'}{\dot{m}C_P}\right)\right]$ (Duffie & Beckman, 2013)

This collector flow factor is a function of the single variable, the dimensionless collector capacitance rate $\frac{\dot{m}C_P}{A_c U_L F'}$ and is shown as

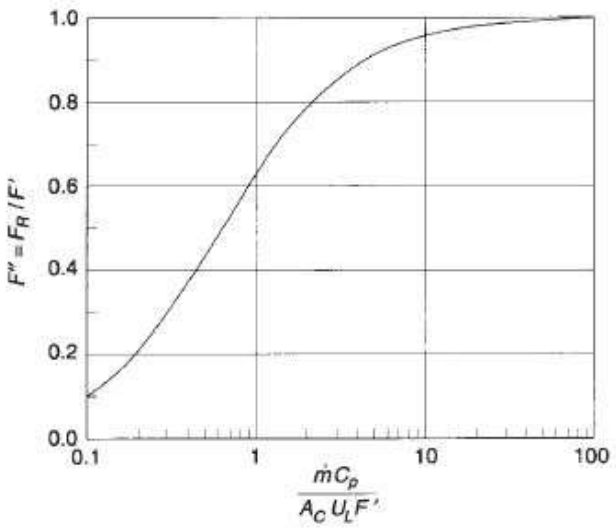

Figure 3.5 Collector flow factor as a function of capacitance rate (Duffie & Beckman, 2013)

The quantity F_R is equivalent to the effectiveness of a conventional heat exchanger, which is defined as the ratio of the actual heat transfer to the maximum possible heat transfer. The maximum possible useful energy gain (heat transfer) in a solar collector occurs when the whole collector is at the inlet fluid temperature; heat losses to the surroundings are then at a minimum. The collector heat removal factor times this maximum possible useful energy gain is equal to the actual useful energy gain

$$Q_u = A_c F_R [S - U_L(T_i - T_a)] \qquad \text{(ASHRAE, 2008)}$$

With it, the useful energy gain is calculated as a function of the inlet fluid temperature. This is a convenient representation when analyzing solar energy systems, since the inlet fluid temperature is usually known. However, losses based on the inlet fluid temperature are too small since losses occur all along the collector from the plate and the plate has an ever-increasing temperature in the flow direction. The effect of the multiplier F_R is to reduce the useful energy gain from what it would have been had the whole collector absorber plate been at the inlet fluid temperature to what actually occurs. As the mass flow rate through the collector increases, the temperature rise through the collector decreases. This causes lower losses since the average collector temperature is lower and there is a corresponding increase in the useful energy gain. This increase is reflected by an increase in the collector heat removal factor FR as the mass flow rate increases.

3.1.9 Mean Fluid and Plate Temperatures

To evaluate collector performance, it is necessary to know the overall loss coefficient and the internal fluid heat transfer coefficients. However, both UL and hfi are to some degree functions of temperature. The mean fluid temperature can be found by integrating

$$T_{fm} = \frac{1}{L}\int_0^L T_f(y)dy$$

Performing this integration and substituting F_R and Q_u from above equations, the mean fluid temperature was shown by Klein et al. (1974) to be

$$T_{fm} = T_{fi} + \frac{Q_u/A_c}{F_R U_L}(1 - F'') \qquad \text{(Klein, 1974)}$$

This is the proper temperature for evaluating fluid properties.

When a collector is producing useful energy, the mean plate temperature will always be greater than the mean fluid temperature due to the heat transfer resistance between the absorbing surface and the fluid. This temperature difference is usually small for liquid heating collectors but may be significant for air collectors.

The mean plate temperature can be used to calculate the useful gain of a collector

$$Q_u = A_c F_R [S - U_L(T_{pm} - T_a)]$$

Then we have

$$T_{pm} = T_{fi} + \frac{Q_u / A_c}{F_R U_L}(1 - F_R)$$

3.1.10 Flow Rate Correction

If a collector is to be used at a flow rate other than that of the test conditions, an approximate analytical correction to $F_R(\tau\alpha)_n$ and $F_R U_L$ can be obtained by following expression assuming that only effect of changing flow rate is to change the temperature gradient in the flow direction and that changes in F' due to changes in h_{fi} are small. The ratio r by which $F_R U_L$ and $F_R(\tau\alpha)_n$ are to be corrected is given by

$$r = \frac{F_R(\tau\alpha)_n|_{use}}{F_R(\tau\alpha)_n|_{test}}$$

$$\text{Or } r = \frac{\frac{\dot{m}C_p}{A_c}[1-\exp\left(-\frac{A_c F' U_L}{\dot{m}C_p}\right)\Big|_{use}}{F_R U_L|_{test}}$$

To use above equations, it is necessary to know or estimate $F'U_L$ which can be calculated as

$$F'U_L = -\frac{\dot{m}C_p}{A_c}\ln\left(1 - \frac{F_R U_L A_C}{\dot{m}C_p}\right) \text{ (Duffie \& Beckman, 2013)}$$

3.2 Analysis of Air Heaters

A schematic diagram of a typical air-heating flat-plate solar collector is shown in Figure 3.6. The air passage is a narrow duct with the surface of the absorber plate serving as the top cover

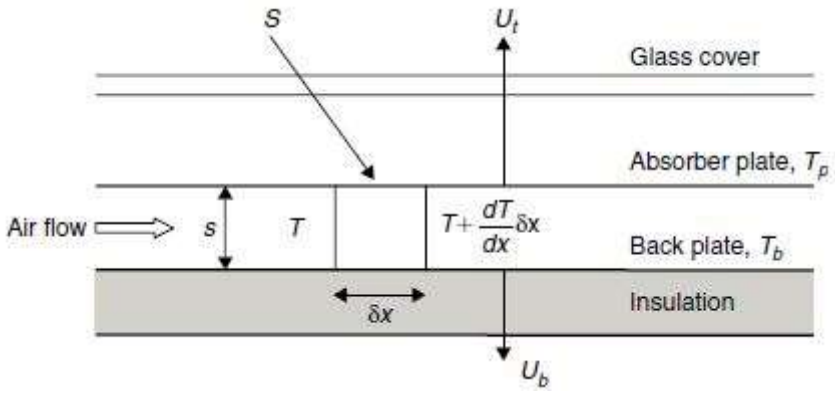

Figure 3.6 Schematic Diagram of Typical Air Heating Collector (Kalogirou, 2006)

F′ collector efficiency factor for air collectors, given by

$F' = \frac{1/U_L}{1/U_L + 1/h}$ where

$h = h_{c,p-a} + 1/(h_{c,b-a} + h_{r,p-b})$

Then the energy gain by the collector is given by

$Q_u = A_c F_R[S - U_L(T_i - T_a)]$ (ASHRAE, 2008)

3.3 Collector Tests

The basic method of measuring collector performance is to expose the operating collector to solar radiation and measure the fluid inlet and outlet temperatures and the fluid flow rate. The useful gain is then

$$Q_u = \dot{m} C_p (T_o - T_i)$$

In addition, radiation on the collector, ambient temperature, and wind speed are also recorded. Thus two types of information are available: data on the thermal output and data on the conditions producing that thermal performance. These data permit the characterization of a collector by parameters that indicate how the collector absorbs energy and how it loses energy to the surroundings.

From above analytical analysis, the thermal performance of a collector operating under steady conditions can be written in terms of the incident radiation:

$$Q_u = A_c F_R[G_t(\tau\alpha) - U_L(T_i - T_a)]$$ (ASHRAE, 2008)

Testing standards generally require that during a collector test the beam normal radiation be high and the diffuse fraction be low. Consequently, the *(τα)* determined under test conditions is for conditions under which a collector provides most of its useful output, that is, when radiation is high and most of the incident radiation is beam radiation.

The above two equations can be used to define an instantaneous efficiency

$$\eta_i = \frac{Q_u}{A_c G_t} = F_R(\tau\alpha) - \frac{F_R U_L(T_i - T_a)}{G_t} = \frac{\dot{m} C_p (T_o - T_i)}{A_c G_t}$$ (Duffie & Beckman, 2013)

The outdoor tests are done in the midday hours on clear days when the beam radiation is high and usually with the beam radiation nearly normal to the collector. Thus the transmittance absorptance product for these test conditions is approximately the normal-incidence value and is written as $(\tau\alpha)_n$

CHAPTER FOUR

EXPERIMENTAL SETUP AND RESULTS

The staggered type solar air heater for testing has been developed by “Sun Works Nepal” that is pioneer company in designing, fabrication and installation of various solar dryers and air heaters. (Refer Appendix III for letter of consent)

Though being utilized as effective Solar Air Heater for various space heating and process heating application, the performance parameters of the collector was unknown till date and need for its performance and efficiency parameters became imperative for considering it in further design process.

The schematic of the collector is presented in the Figure 4.1 below:

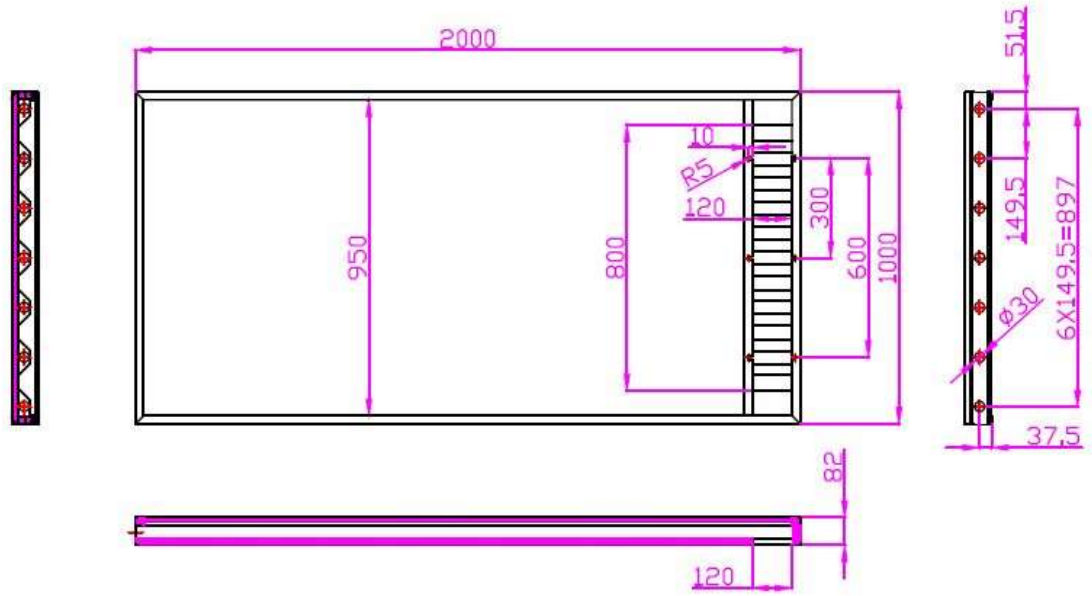

Figure 4.1 Details of Solar Collector (Manufacturer: Sun Works Nepal)

The absorber is of staggered type Aluminum plate with Black Chrome Selective Coating. The collector frame is designed with Anodized Aluminum Profile and the glazing utilized is Low Iron, Toughened, and Patterned Glass. High density thermocole Styrofoam insulation is used as an insulation.

Figure 4.2 Staggered Type Solar Air Heater

4.1 Instrumentation and Experimental Setup

A schematic view of the SAH is presented. The AC blower San Ace 172 and Sunon DP200A is fitted at end of the collector for the required flow rate. Two thermometers were fitted, one at inlet and one at outlet to measure the inlet and outlet temperature. The outlet air velocity was measured by Anemometer (AR826) at the outlet of the blower from which flowrate was calculated. The solar radiation was measured by handheld pyranometer from SOLDATA 98 HP. The ambient temperature was measured by normal mercury thermometer. U-tube manometer is utilized to measure the pressure drop from inlet to outlet. The angle is modified by providing various steps to the support structure.

The lists of instruments are:

1 Pyranometer (Soldata 98 HP)

2. Anemometer (Smart Sensor AR826)

4. AC blower (San Ace 172)

5. U-tube Manometer

6. Mercury Thermometers

Figure 4.3 Test Setup with AC blower connected at the outlet of SAH

Various types of support structure were used to setup the inclination angle and assembly for the blower attachment was changed to test the collector in lower flowrate. Data sheet of blowers used in the test and additional photographs of test setups are presented in Appendix III, through Appendix VII.

The test data were recorded manually in each 20 minutes interval and the test started from 10 am in the morning to 5 pm in the evening. The total uncertainty in determining flow rate, efficiency and $\frac{(T_{a,in}-T_{amb})}{G_t}$ are calculated as 3%, 8.2 % and 7 % respectively. (Refer Appendix VI)

4.2 Results and Discussions

The test was carried out on 8th, 9th and 10th of September at constant mass flow rate of 0.0645 kg/s. The incidence angle was changed as 37 ^{0} , 27 ^{0} and 17 ^{0} respectively on the 6th , 7th and 8th of September. Then the flow rate was reduced to 0.0344 kg/s with respective incidence angle of 37 ^{0} and 27 ^{0} on 9th & 10th of September. All the graphs and figures from Figure 10 to Figure 16 are generated from the experimental testing and analysis of the data thus obtained. Refer Appendix V for the useful energy collected by the collected in the test days.

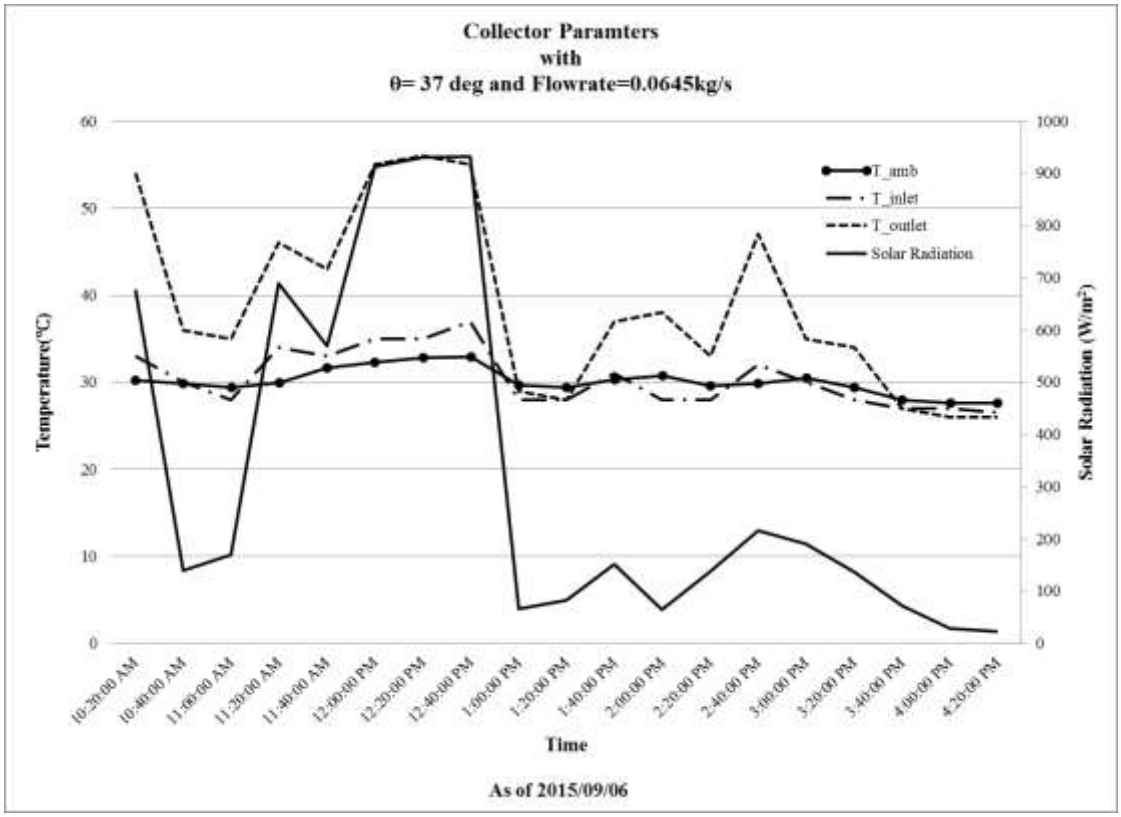

Figure 4.4 Collector Performance as of 2015/09/06

Figure 4.4 shows the variation of ambient temperature, inlet temperature, outlet temperature and solar radiation in each 20 min interval at constant mass flow rate of 0.0645 kg/s and at incidence angle of 37 degrees. The highest daily solar radiation obtained is 932 W/m^2, during which ambient, inlet and outlet temperature were also recorded highest as 32.9 ℃ , 37 ℃ and 66 ℃ respectively. The solar radiation decreased drastically from 1:00:00 pm due to increasing cloud cover with the solar radiation as low as 22 W/m^2. The pressure drop measured on the collector was 4 mm of WC. The useful energy collected during the day was calculated as 10.45 MJ.

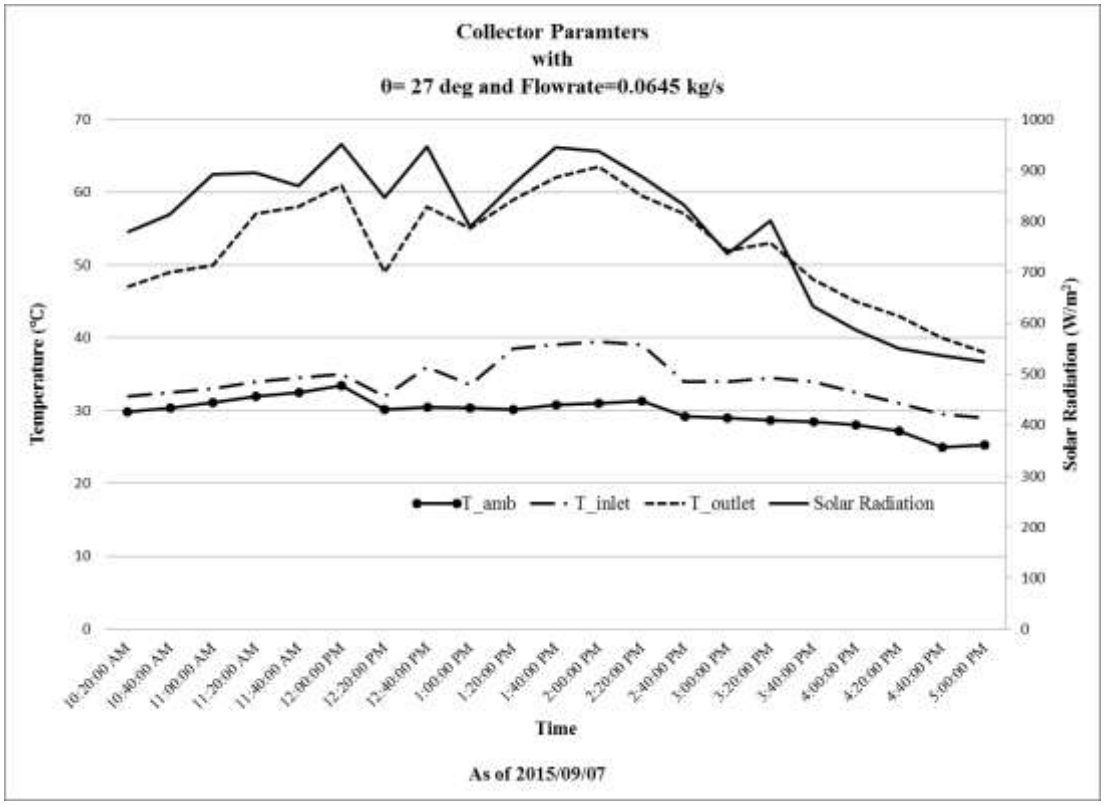

Figure 4.5 Collector Performance as of 2015/09/07

Figure 4.5 shows the variation of ambient temperature, inlet temperature, outlet temperature and solar radiation in each 20 min interval at constant mass flow rate of 0.0645 kg/s and at incidence angle of 27 degrees. The highest daily solar radiation obtained is 946 W/m^2, during which ambient temperature was recorded highest as 33.4 ℃. The maximum inlet and outlet temperature occurred as 39 ℃ and 63.5 ℃ when there were uniform high solar radiation of above 900 W/m^2 around 12:00:00 to 1:00:00 pm .The solar radiation gradually decreased after that but maintained a value minimum of 525 W/m^2 due to good sunshine in the experiment day. The pressure drop measured on the collector was 3 mm of WC. The useful energy calculated during the day was calculated as 28 MJ.

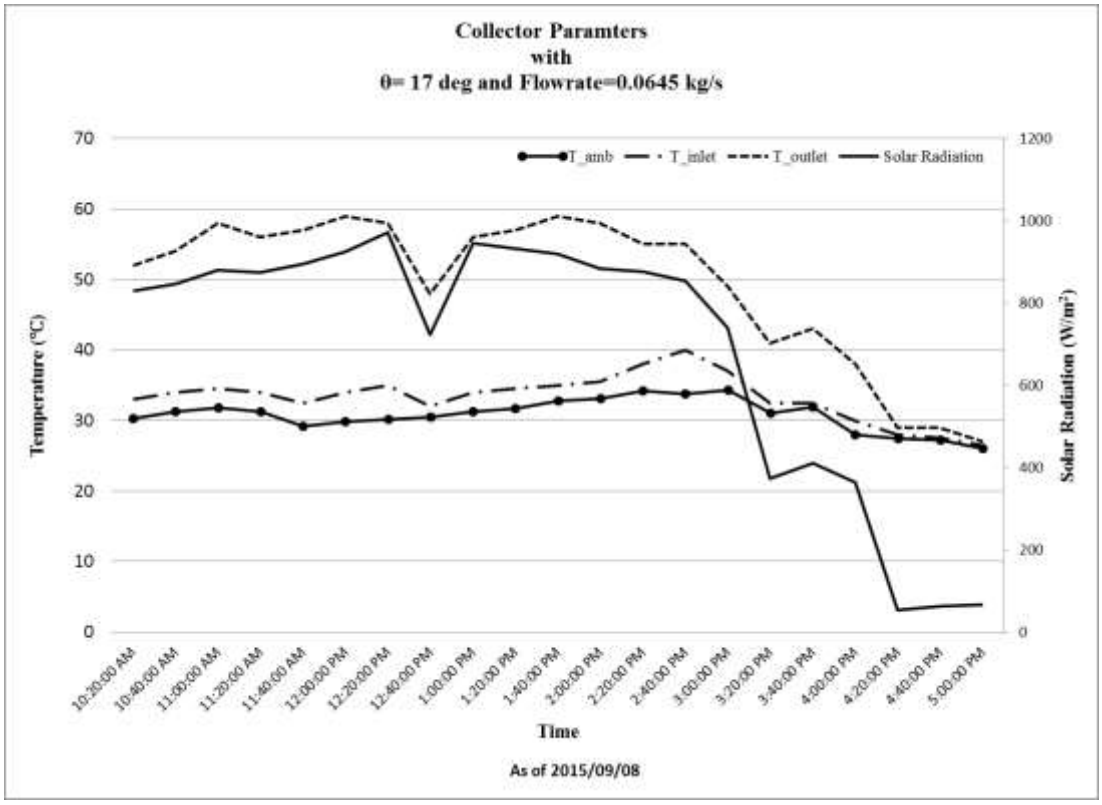

Figure 4.6 Collector Performance as of 2015/09/08

Figure 4.6 shows the variation of ambient temperature, inlet temperature, outlet temperature and solar radiation in each 20 min interval at constant mass flow rate of 0.0645 kg/s and at incidence angle of 17 degrees. The highest daily solar radiation obtained is 972 W/m^2, during which ambient temperature was recorded as 30.2 ℃. The maximum ambient, inlet and outlet temperature occurred as 34.3 ℃, 40 ℃ and 59 ℃ when there were uniform high solar radiation of above 800 W/m^2 around 12:00:00 to 1:00:00 pm. The solar radiation gradually decreased and then significantly after 3:00:00 pm due to cloud cover during experiment day. The pressure drop measured on the collector was 2.5 mm of WC. The useful energy collected during the day was calculated as 26.08 MJ.

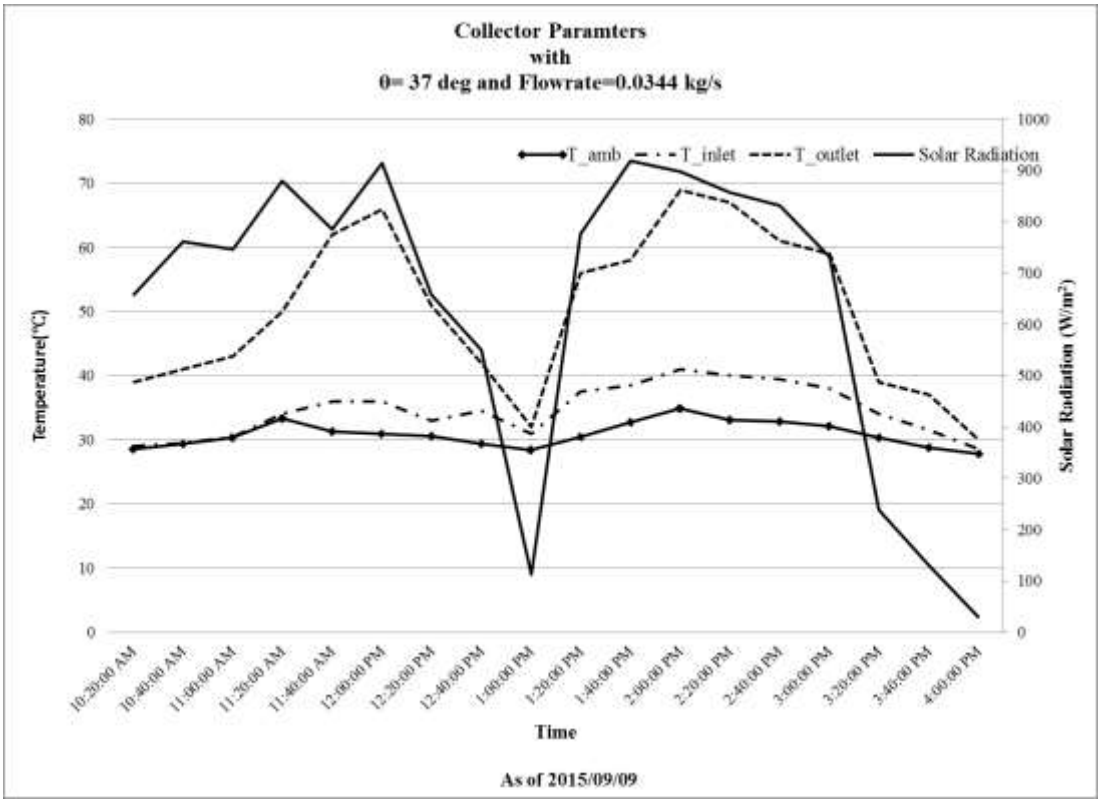

Figure 4.7 Collector Performance as of 2015/09/09

Figure 4.7 shows the variation of ambient temperature, inlet temperature, outlet temperature and solar radiation at constant and reduced mass flow rate of 0.0343 kg/s and at incidence angle of 37 degrees. The highest daily solar radiation obtained is 919 W/m^2, around the periphery of which ambient temperature was recorded as 34.9 ℃. and maximum outlet temperature reaching 69 ℃. The maximum inlet temperature recorded was 41 ℃ around 2 pm. The solar radiation showed drastic drop during 1:00 pm due to complete cloud cover thereby reducing all the measured temperatures to the minimum. The pressure drop measured on the collector was 6 mm of WC which is significant due to reduced flow rate and reduced turbulence in the ducts. The useful energy collected during the day was 10.63 MJ.

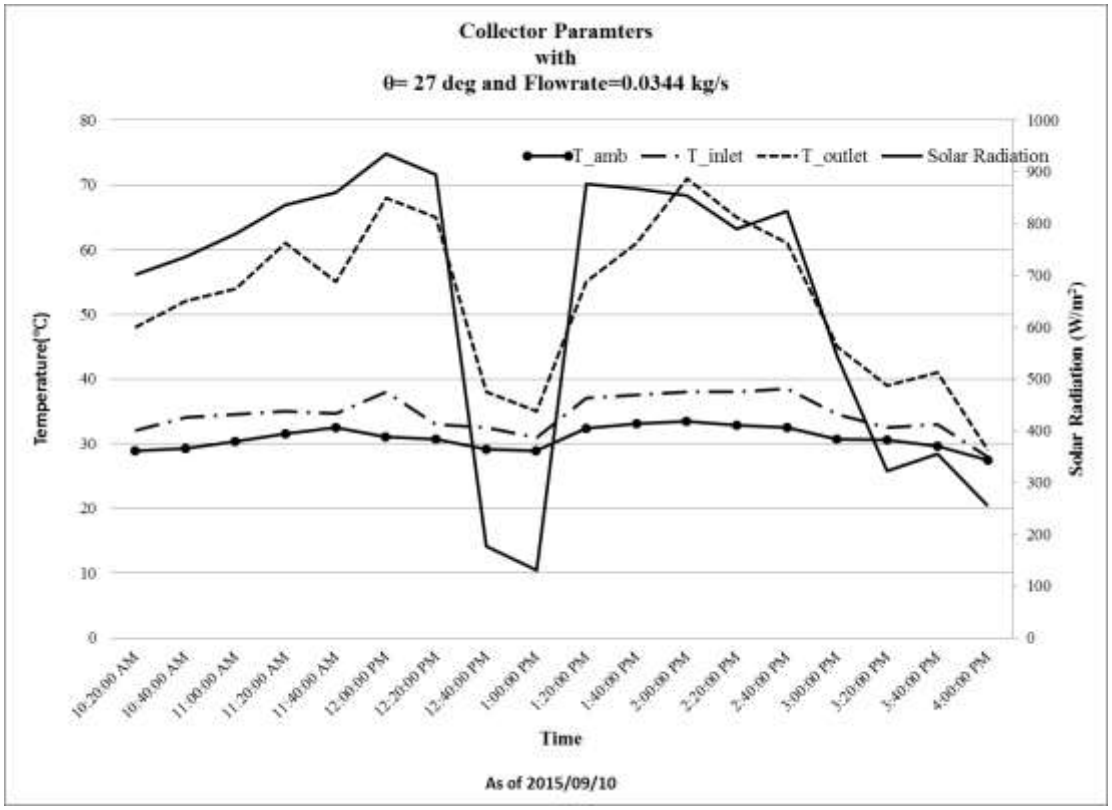

Figure 4.8 Collector Performance as of 2015/09/10

Figure 4.8 depicts the measured ambient, inlet and outlet temperatures alongside the corresponding solar radiation. Besides rapid decrease in solar radiation during 1:00 pm for brief period of time, the day had good amount of solar radiation with maximum radiation reaching up to 935 W/m^2 at noon. The outlet temperature reached maximum around 2:00 pm with constant radiation of greater than 750 W/m^2 around 1:20 to 2:00 pm with values reaching up to 71℃ . Similarly the corresponding ambient and outlet temperatures were maximum at that period. The pressure drop measured on the collector was 5 mm of WC. The useful energy collected during the day was 13.19 MJ.

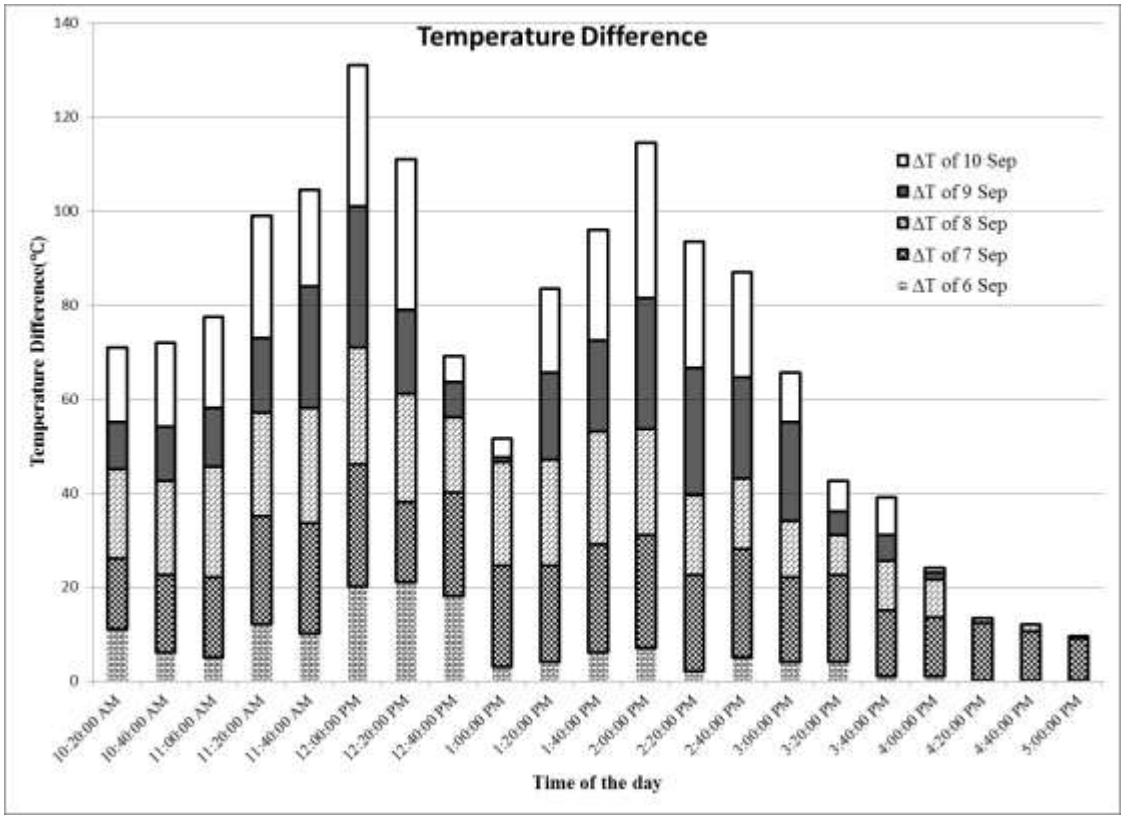

Figure 4.9 Temperature Difference between Outlet and Inlet Temperatures

Figure 4.9 shows the temperature difference between outlet and inlet temperatures on the different experiment days. The maximum and significant temperature difference were recorded during 10th September and 9th September; during days in which experiment were conducted with reduced flow rate of 0.0344 kg/s than that compared to other days in which the experiment was conducted at flow rate of 0.0645 kg/s.

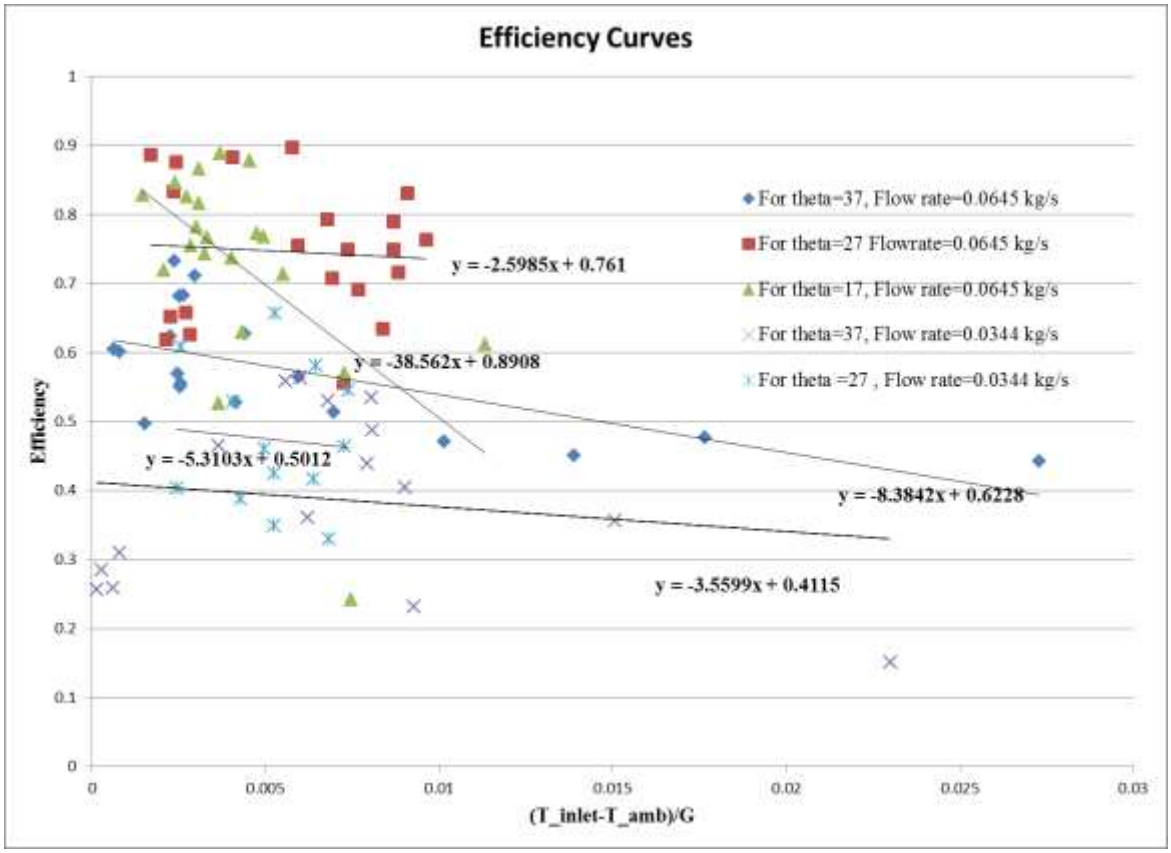

Figure 4.10 Efficiency Curves for Different angle of incidence

Figure 4.10 shows the efficiency for different angle of incidence in the collector by least-square fitting of the experimental data. The efficiency of test data can be summarized as:

For mass flow rate of $\dot{m}$ = 0.0645 kg/s,

$$\eta_{17deg.} = 0.8908 - \frac{38.56(T_i - T_a)}{G_t}$$

$$\eta_{27deg.} = 0.761 - \frac{2.5985(T_i - T_a)}{G_t}$$

$$\eta_{37deg.} = 0.6228 - \frac{8.3842(T_i - T_a)}{G_t}$$

From above graph even though the highest efficiency intercept is obtained for the 17 degree inclination angle, the slope of the equation is steep so effective for instantaneous efficiency but not promising for more energy collection. The efficiency intercept at the 27 degrees angle of incidence is 0.761 and slope is also very less steep so making in a good alternative for using in different ranges of inlet temperature

without significant drop in the efficiency. Also the intercept at the 37 degrees incidence angle is low and also more slope than that of 17 degree equation so overall efficiency of the system is lowered.

With significant slope for the 17 degree inclination angle being too pronounced in decreasing the efficiency, further tests at reduced flowrate was avoided.

For mass flow rate of $\dot{m}$ = 0.0343 kg/s,

$$\eta_{27deg.} = 0.5012 - \frac{5.3103(T_i - T_a)}{G_t}$$

$$\eta_{37deg.} = 0.4115 - \frac{3.5599(T_i - T_a)}{G_t}$$

The efficiency is more when the flow rate in the collector is high due to higher turbulence created in the collector than at the reduced flow rate. The optimum operating point for the collector at 0.0645 kg/s is at 27 degree angle of incidence with maximum efficiency of 76.1 % and at 0.0344 kg/s is at 27 degree angle of incidence with maximum efficiency of 50.12 %.

In order to make the comparison for the thermal performance of staggered type, black chrome coated aluminum absorber plate, following configurations of SAHs reported in literature were selected. Hernandez, 2013 analytically studied the thermal behaviour of solar air heaters of double-parallel flow and double-pass counter flow at the flow rate of 0.04 kg/s. Filiz Ozgen, 2009 experimentally investigated the thermal performance of a double-flow solar air heater having aluminum cans for mass flow rates of 0.03 kg/s and 0.05 kg/s.

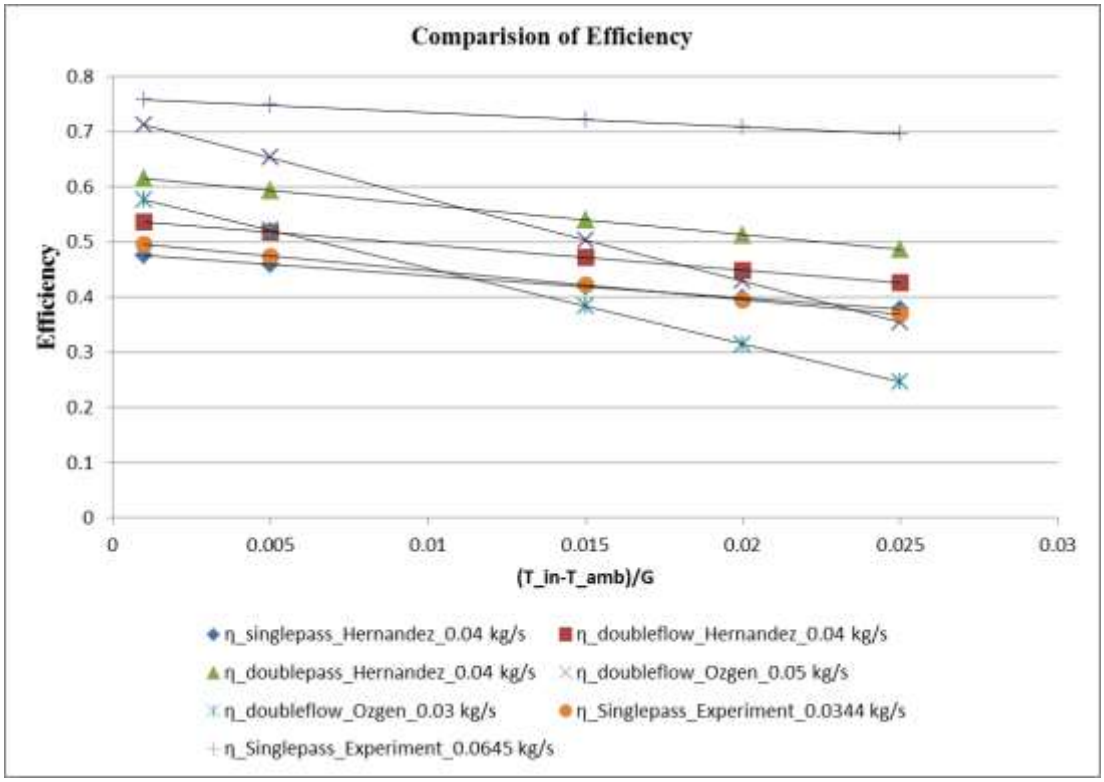

Figure 4.11 Comparison of thermal efficiency of the experimented absorber with reported ones

Figure 4.11 depicts the good agreement of efficiency of the staggered plate absorber plate Solar Air heater with reported literatures. The greater efficiency at the greater flow rate of 0.0645 kg/s is obvious due to increase turbulence in the collectors as well as increase in collector heat removal factor F_R.

The performance parameters of the staggered type Solar Air Collector was measured experimentally and the collector performed better on higher flow rate of 0.0645 kg/s at collector slope of 27 degrees. By ascertaining the performance parameters for the collector, it becomes now effective for utilization in various designs where the need of the Solar Air Collector is felt. On both the flow rates, the collector showed maximum efficiency when the collector angle was set at 27 degrees due to normal incidence of sunlight

CHAPTER FIVE

PEBBLE BED ENERGY STORAGE SYSTEM

A packed-bed (also called a pebble bed or rock pile) storage unit uses the heat capacity of a bed of loosely packed particulate material to store energy. A fluid, usually air, is circulated through the bed to add or remove energy. A variety of solids may be used, rock being the most widely used material. When solar radiation is available, hot air from the collectors enters the top of the storage unit and heats the rocks. As the air flows downward, heat transfer between the air and the rocks results in a stratified distribution of the pebbles, having a high temperature at the top and a low one at the bottom. This is the charging mode of the storage unit. When there is heating demand, hot air is drawn from the top of the unit and cooler air is returned to the bottom of the unit, causing the bed to release its stored energy. This is the discharge mode of the pebble bed storage unit. (Kalogirou, 2006)

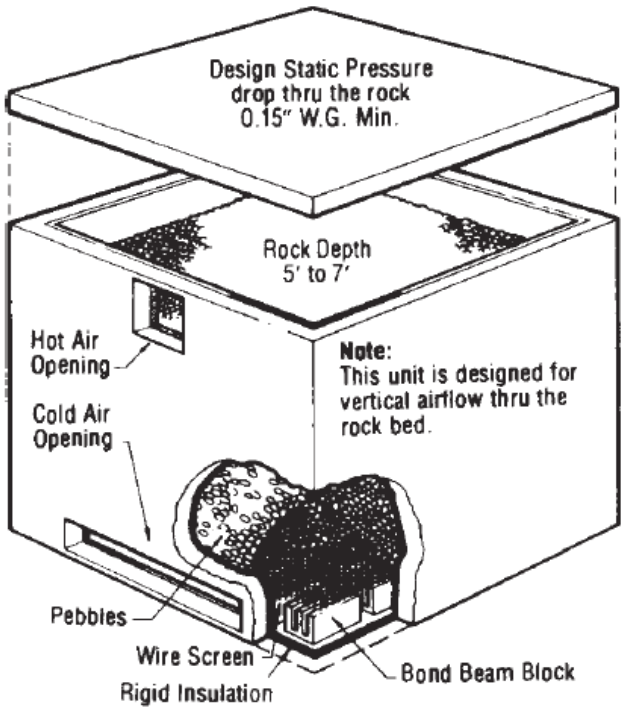

Figure 5.1 A Sample Rock Bed Storage Unit (Duffie & Beckman, 2013)

The heat transfer coefficient between the air and solid is high, which promotes thermal stratification; the costs of the storage material and container are low; the conductivity of the bed is low when there is no airflow; and the pressure drop through

the bed can be low making pebble bed storage as an attractive option for the storage of solar energy.

The high heat transfer coefficient–area product between the air and pebbles means that high-temperature air entering the bed quickly loses its energy to the pebbles. The pebbles near the entrance are heated, but the temperature of the pebbles near the exit remains unchanged and the exit air temperature remains very close to the initial bed temperature.

When the bed is fully charged, its temperature is uniform. Reversing the flow with a new reduced inlet temperature results in a constant outlet temperature at the original inlet temperature for 5 h and then a steadily decreasing temperature until the bed is fully discharged. (Duffie, 2013)

Boxes containing uniformly sized pebbles or stones are typically used as the basic component of thermal storage subsystems of solar space heating systems. During storage of excess thermal energy, heated air is routed to the top of the pebble bed. Air passes downward through spaces between pebbles and transfers thermal energy to the pebbles.

Because of the large exposed surface area of pebbles and limited physical contact, pebble beds are progressively heated from top to bottom. This provides good vertical temperature stratification within the bed. Exit air temperatures from the bottom of the bed are usually at or near room temperature. The low air temperature returning to the collectors is ideal because collectors will operate at near-optimum thermal efficiency. (ASHRAE Design Manual)

Thermal Performance of Packed Bed System

Thermal performance of a packed bed is concerned with heat transfer from flowing air to solid material packed in a container and vice versa. The rate of heat transfer to or from the storage material elements in a packed bed is a function of physical properties of air and solid, local temperature of air and surface of material elements, mass flow rate of air and characteristics of the packed bed. The bed may be arranged in an orderly or randomly fashion. Random packing is the most common arrangement and results when particles of the same approximate size and shape are packed in a container. The characteristics of the packed bed are dependent upon the shape and

orientation of the storage material elements and void fraction of the bed. Heat transfers between air and solid through a complex mechanism. Major resistance to heat transfer takes place at the interface of air and solid and is inversely proportional to the convective heat transfer coefficient. Rise in temperature of material elements is dependent upon transient heat conduction from surface to interior of the solid. It also depends, to a lesser degree, on inter-particle conduction of heat when the adjacent material element comes in direct physical contact. Transfer of heat through the container walls also influences performance of the packed bed. Another factor influencing the rate of heat transfer is mixing action within the air that results from eddies created as the fluid flows through the complex set of flow passages. (Singh, et al., 2009)

The physical characteristics of pebbles vary widely between samples. Three quantities have been used to describe pebbles, the average particle diameter *D*, the void fraction ε, and the surface area shape factor α.

The density of the rock material is then

$$\rho_r = \frac{m}{V(1-\varepsilon)}$$

The Pressure Drop Characteristics of the pebble bed is given by the relationship developed by Dunkle and Ellul (1972)

$$\Delta p = \frac{LG_o^2}{\rho_{air} D}\left(21 + 1750\frac{\mu}{G_o D}\right)$$

where *Go* is the mass velocity of the air (air mass flow rate divided by the bed frontal area) and *L* is the length of the bed in the flow direction

The volumetric heat transfer coefficient is then calculated as

$$h_v = 650\left(\frac{G_0}{D}\right)^{0.7} \qquad \text{(Duffie \& Beckman, 2013)}$$

where h_v is the volumetric heat transfer coefficient in W/m^3 K, *Go* is the mass velocity in kg/m^2 s, and *D* is the particle diameter in meters. The relationship between volumetric heat transfer coefficient *hv* and area heat transfer coefficient *h* is

$$h_v = 6h(1-\varepsilon)\frac{\alpha}{D} \text{ (Duffie \& Beckman, 2013)}$$

Considering the assumption for the analytical study as carried out by Schumann(1929) like one are one-dimensional plug flow, no axial conduction or dispersion, constant properties, no mass transfer, no heat loss to the environment, and no temperature gradients within the solid particles. The differential equations for the fluid and bed temperatures are

$$\left(\rho C_p\right)_f \epsilon \frac{\partial T_f}{\partial t} = -\frac{\left(\dot{m} C_p\right)}{A}\frac{\partial T_f}{\partial x} + h_v(T_b - T_f)$$

$$\left(\rho C_p\right)_b (1-\epsilon)\frac{\partial T_b}{\partial t} = h_v(T_f - T_b)$$

where ε is the bed void fraction, hv is the volumetric heat transfer coefficient between the bed and the fluid (i.e., the usual area heat transfer coefficient times the bed particulate surface area per unit bed volume), and other terms have their usual meanings

For an air-based system, the first term on the left-hand side of can be neglected and the equations can be written as

$$\frac{\partial T_f}{\partial (x/L)} = NTU(T_b - T_f)$$

$$\frac{\partial T_b}{\partial \theta} = NTU(T_f - T_b)$$

$$NTU = \frac{h_v AL}{\left(\dot{m} C_p\right)_f}$$

And the dimensionless time is

$$\theta = \frac{t\left(\dot{m} C_p\right)_f}{\left(\rho C_p\right)_b (1-\epsilon) AL}$$ (Duffie & Beckman, 2013)

where A is bed cross-sectional area and L is bed length. Analytical solutions to these equations exist for a step change in inlet conditions and for cyclic operation.

CHAPTER SIX

INTEGRATION OF STAGGERED TYPE SAH WITH PEBBLE BED ENERGY STORAGE

A schematic of a basic solar air heating system, with a pebble bed storage unit and an auxiliary heating source, is shown in Figure 6.1

In this case, the various operation modes are achieved by the use of the dampers shown. Usually, in air systems, it is not practical to have simultaneous addition and removal of energy from the storage. If the energy supplied from the collector or the storage is not adequate to meet the load, auxiliary energy can be used to top up the air temperature to cover the building load. When there is no sunshine and the storage tank is completely depleted, it is also possible to bypass the collector and the storage unit and use the auxiliary alone to provide the required heat

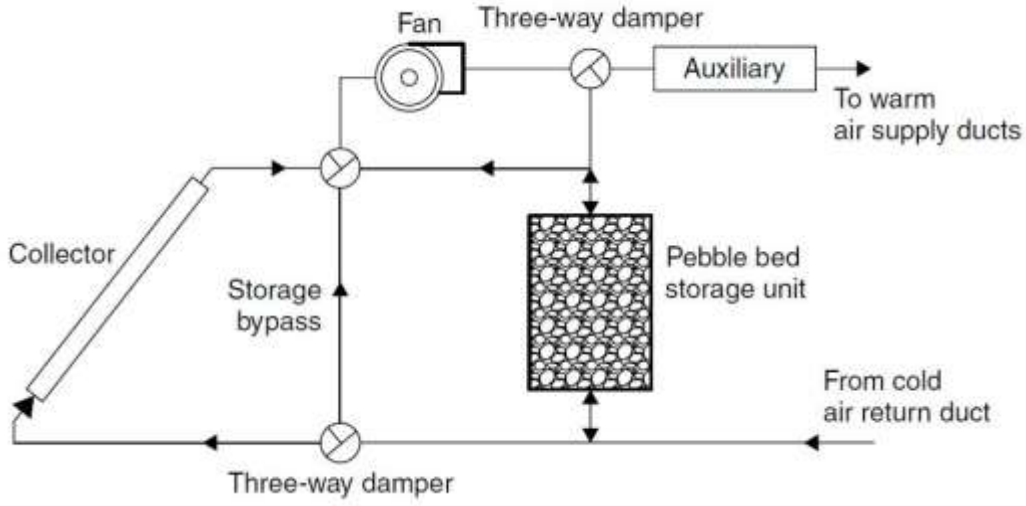

Figure 6.1 Schematic of Basic Solar Energy Storage and Heating System (Kalogirou, 2006)

6.1 System Configuration

The proposed system as shown in Figure 6.2 includes a staggered type Solar Air heater which heats the circulating air through solar irradiation, and transfer the heat to the pebble bed. The pebble bed is charged during the sunshine hours. When the radiation level is low and heat is required in the room, the air enters the pebble bed at the bottom and heats the space.

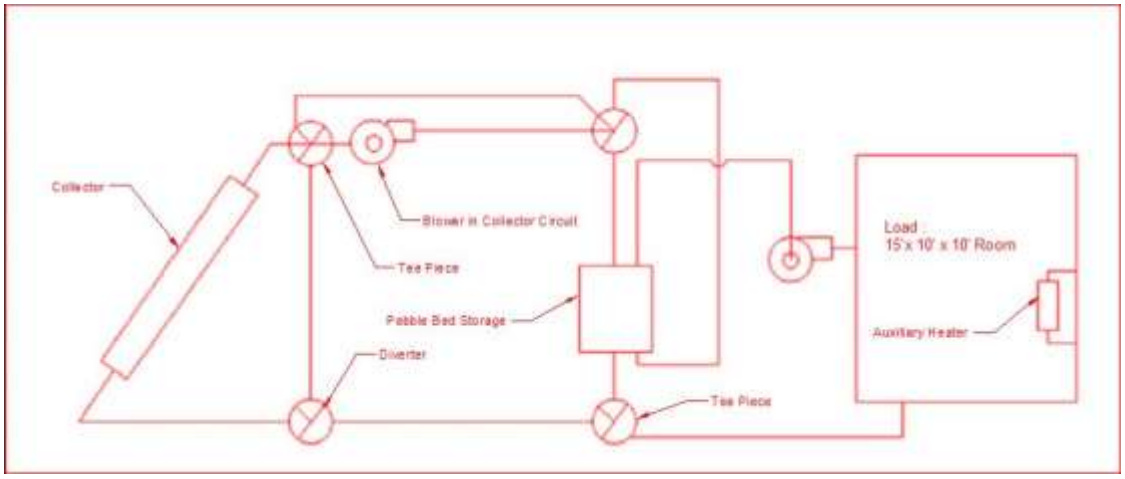

Figure 6.2 Schematic of the Proposed System

The system operates on three mode of operation as

- If the solar energy is available then energy gain from the collector is used to charge the pebble bed
- If the heating is required in the room during off sunshine hours, heating the room from the energy stored in the pebble bed
- Heat from the auxiliary source is supplied whenever there is deficit in the energy supplied form the pebble bed to maintain the room temperature to the set temperature

The system model is designed to provide the heating needs of a living dwelling of the general type of room of the houses of the Kathmandu Valley. In order to use solar air heating of a building at times that do not coincide with the solar radiation, the heat must then be stored. This plays a very important role, particularly in dwellings, as heat is required in the evening and at night.

A sample schematic of such room is presented below

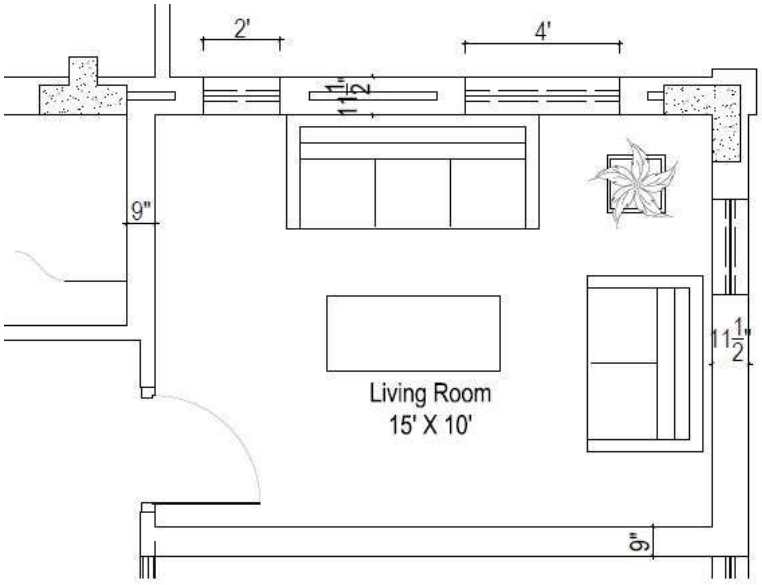

Figure 6.3 Schematic of a Sample heating Room

The room consists of two 11.5''(0.2921 m) wall with plaster on both sides on the outer with total effective windows opening of are 32 sq. ft. Two 9 inch (0.2286 m) (inner walls with plaster on each side surrounds the room.

Table 6.1 UA Value Calculation for Typical Room

Description	**U Value (BTU/hr ft^2 F)**	**Area (sq. ft.)**	**UA (BTU/hr F)**
Floor	0.12	150	18
Ceiling (Concrete Slab)	0.29	150	43.5
Window (Single Glazing)	0.51	32	16.32
Wall (9 and 11.5 in wall with plaster on both sides)	0.44	468	205.92
	(Pita, 2009)		**283.74 (150 W/K)**

6.1.1 Weather of Kathmandu

The proposed system is designed to meet the heating load during the heating months October, November, December, January, February and March where the heating degree days value are significant and the average air temperature is low thus depicting the need of the heating requirements.

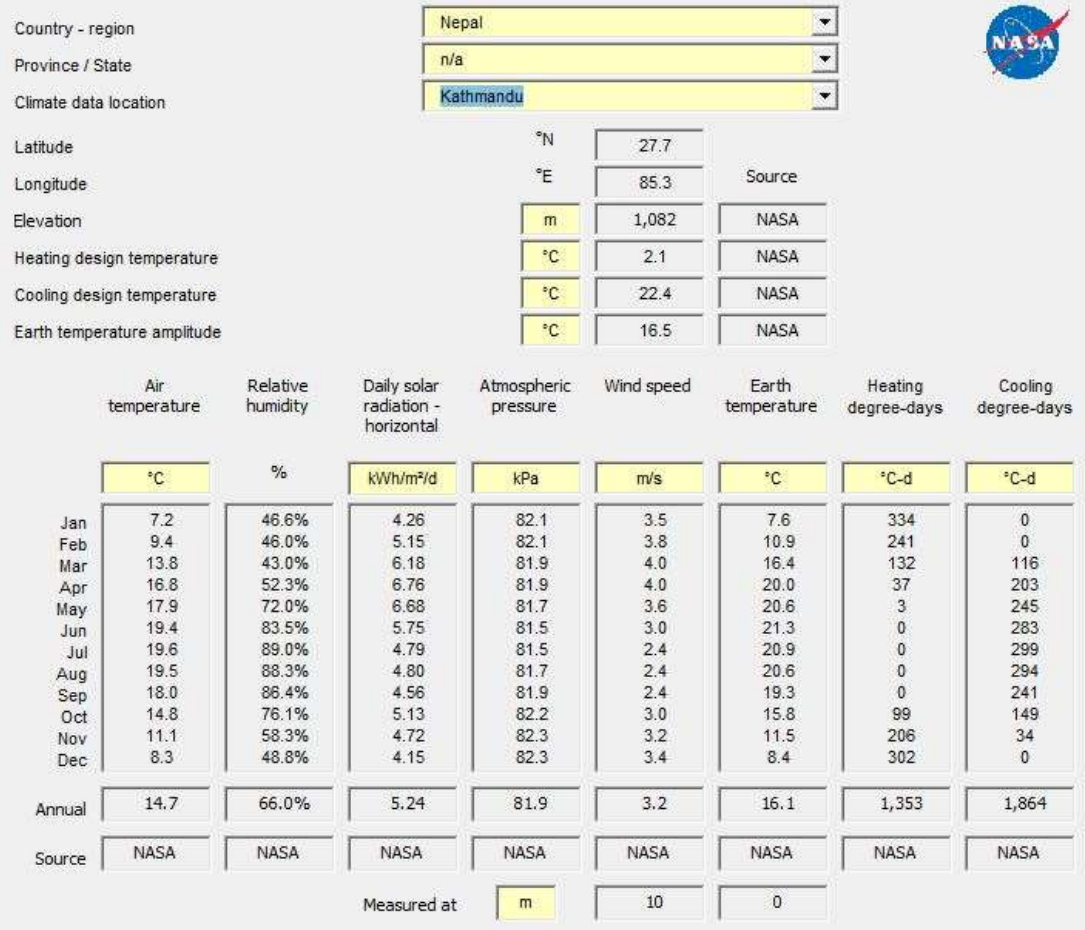

Country - region	Nepal		
Province / State	n/a		
Climate data location	Kathmandu		
Latitude	°N	27.7	
Longitude	°E	85.3	Source
Elevation	m	1,082	NASA
Heating design temperature	°C	2.1	NASA
Cooling design temperature	°C	22.4	NASA
Earth temperature amplitude	°C	16.5	NASA

	Air temperature	Relative humidity	Daily solar radiation - horizontal	Atmospheric pressure	Wind speed	Earth temperature	Heating degree-days	Cooling degree-days
	°C	%	kWh/m²/d	kPa	m/s	°C	°C-d	°C-d
Jan	7.2	46.6%	4.26	82.1	3.5	7.6	334	0
Feb	9.4	46.0%	5.15	82.1	3.8	10.9	241	0
Mar	13.8	43.0%	6.18	81.9	4.0	16.4	132	116
Apr	16.8	52.3%	6.76	81.9	4.0	20.0	37	203
May	17.9	72.0%	6.68	81.7	3.6	20.6	3	245
Jun	19.4	83.5%	5.75	81.5	3.0	21.3	0	283
Jul	19.6	89.0%	4.79	81.5	2.4	20.9	0	299
Aug	19.5	88.3%	4.80	81.7	2.4	20.6	0	294
Sep	18.0	86.4%	4.56	81.9	2.4	19.3	0	241
Oct	14.8	76.1%	5.13	82.2	3.0	15.8	99	149
Nov	11.1	58.3%	4.72	82.3	3.2	11.5	206	34
Dec	8.3	48.8%	4.15	82.3	3.4	8.4	302	0
Annual	14.7	66.0%	5.24	81.9	3.2	16.1	1,353	1,864
Source	NASA	NASA	NASA	NASA	NASA	NASA	NASA	NASA
			Measured at	m	10	0		

Figure 6.4 Climatic Data of Kathmandu (NASA/Retscreen Software)

The system being proposed is developed to maintain the room temperature of 20 degree centigrade during all the time.

6.1.2 Solar Air Collector

For the solar heating of a building the primary system design variable is collector area, with storage capacity and other design variables being of secondary importance provided they are within reasonable bounds of good design practice.

The Solar Air Collector forms the most important component for the Solar Air Heating System and its performance greatly affects the overall performance of the system. The Solar Air Heater being considered for the proposed model was experimentally tested in the testing setup as discussed previously and its performance parameters were ascertained.

The experimental test on the collector at inclination angle of 27 degrees and the flow rate of 0.0645 kg/s yielded the value of $F_R(\tau\alpha)$ = 0.76 which is the product of

collector heat removal factor and product of transmittance and absorptance at normal incidence and $F_R U_L = 2.59$ which is the collector heat removal factor and collector overall heat loss coefficient. Similarly, with the collector kept at the same inclination which is the optimum collector slope for the location, and the flow rate being reduced to 0.0344 kg/s yielded $F_R(\tau\alpha)$ = 0.41 and $F_R U_L = 3.56$.

6.1.3 Pebble Bed Energy Storage

The pebble bed storage is designed with the recommended values published in various literatures. The recommended design parameters for the bed length in which flow direction occurs is recommended 1.25-2.5 m, whereas the pebble size should have 0.01-0.03 m with storage capacity 0.15-0.35 m^3 pebbles/m^3. The pressure drop in the pebble bed is required to be kept as minimum as 55 Pa. The void fraction is recommend to the values of 0.3-.05 (Duffie & Beckman, 2013)

As per the space being considered for the heating the length of the bed is kept to 1.5 m and cross sectional area to 0.82 x 0.82 m^2 . The void fraction is kept at 0.4 which results in the apparent rock bed density of 1800 kg/m^3.

6.2 Simulation Setup

Simulations of the certain systems offer the opportunity to determine the effects of changes in system configuration and design parameters and changes in climate on annual performance. Simulations are uniquely suited to parametric studies and thus offer to the process designer the capability to explore the effects of design variables on long-term system performance. They offer the opportunity to evaluate effects of system configuration and alternative system concepts. They have the advantage that the weather used to drive them is reproducible, allowing parametric and configuration studies to be made without uncertainties of variable weather.

6.2.1 TRNSYS: Thermal Process Simulation Program

TRNSYS is an acronym for “transient simulation,” which is a quasi-steady simulation model. This program was developed at the University of Wisconsin by the members of the Solar Energy Laboratory and written in the FORTRAN computer language. The program consists of many subroutines that model subsystem components. The

mathematical models for the subsystem components are given in terms of their ordinary differential or algebraic equations. With a program such as TRNSYS, which Modeling and Simulation of Solar Energy Systems can interconnect system components in any desired manner, solve differential equations, and facilitate information output, the entire problem of system simulation reduces to a problem of identifying all the components that make up the particular system and formulating a general mathematical description of each (Kalogirou, 2004b).

Subsystem components in the TRNSYS include solar collectors, differential controllers, pumps, auxiliary heaters, heating and cooling loads, thermostats, pebble bed storage, relief valves, hot water cylinders, heat pumps, and many more. There are also subroutines for processing radiation data, performing integrations, and handling input and output. Time steps down to 1/1000 hour (3.6 s) can be used for reading weather data, which makes the program very flexible with respect to using measured data in simulations. Simulation time steps at a fraction of an hour are also possible.

The DLL-based architecture allows users and third-party developers to easily add custom component models, using all common programming languages (C, C++, PASCAL, FORTRAN, etc.) In addition, TRNSYS can be easily connected to many other applications, for pre- or post-processing or through interactive calls during the simulation (e.g. Microsoft Excel, Matlab, COMIS, etc.). TRNSYS applications include:

Solar systems (solar thermal and PV), Low energy buildings and HVAC systems with advanced design features (natural ventilation, slab heating/cooling, double façade, etc.), Renewable energy systems, Cogeneration, fuel cells etc.

The proposed model is developed in the TRNSYS as follows

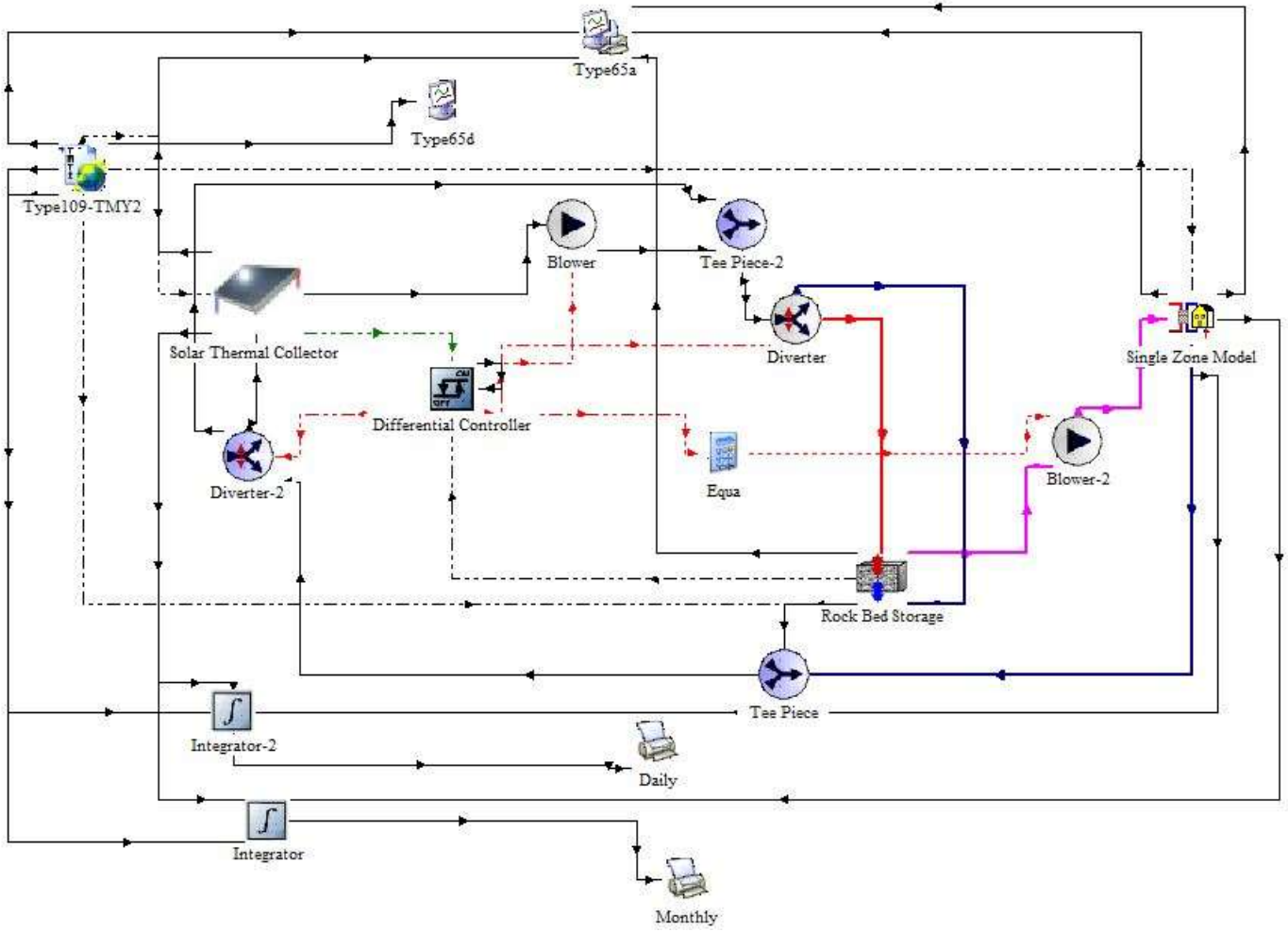

Figure 6.5 Model in TRNSYS Simulation Studio

6.3 Description of the Components

The input output parameters and the mathematical reference pertaining to following components is presented in Appendix II

Solar Collector

The Solar Collector utilized in the model is Type 1a model with the parameters set as obtained from the experimental results. The $F_R(\tau\alpha)$ and $F_R U_L$ value was set as .761 and 2.59 when the model was simulated with 0.0645 kg/s and .50 and 5.31 for the flow rate of 0.0344 kg/s.

Weather Data

The weather data for Kathmandu was utilized form the data provided by TRNSYS software. The data file distributed with TRNSYS 16 were generated using Meteonorm which interpolates hourly weather files where actual reading of solar radiation is not available.

Storage Bed

The model used for pebble bed is Type 10 component in TRNSYS. The bed allows only one directional flow at a time, either from top to bottom or from bottom to top. The bed was divided into 5 nodes to study the proper temperature distribution.

The parameters were set as follows

Table 6.2 Parameters for the Pebble Bed Storage

Parameters Description	Values
Specific Heat of Air	1.005 (KJ/kgK)
Length of Rock Bed	1.5 m
Cross Sectional Area	0.67 m^2
Perimeter	3.24 m
Specific Heat of Rock	0.9 KJ/kgK
Apparent Rock Bed Density	1800 kg/m^3
Loss Coefficient	3 KJ/hr m^3K
Effective Thermal Conductivity	10 KJ/hr m K

Single Zone Load Structure

The room was modeled as single zone load structure with type 12a of the TRNSYS type. The parameters were set as follows:

Table 6.3 Parameters for Single Zone Load Structure

Overall Conductance	284 (BTU/hr F) (150 W/K)
House Set Point Temperature	20 deg C
Flow Rate When Pump is Operating	700 kg/hr
Effective Cmin Product	700 KJ/hrK

Blower

Two blower were used in the circuit. Blower 1 is used for the solar collector loop when the solar radiation is available and pebble bed is being charged. Blower 2 supplies higher flow rate air of 700 kg/hr to the house to meet the heating load. The controller signal is utilized to alternate the operation of the blower.

Controller

An on/off differential controller that generates the on/off signals was utilized to operate the blowers and the diverter. The lower input and monitoring temperature was the average temperature of pebble bed, and outlet temperature of the collector was utilized as the upper input temperature. The Upper dead band temperature was set to 10 deg C and lower dead band to 2 deg C.

CHAPTER SEVEN

SIMULATION RESULTS

The results obtained form the simulation are presented as follows

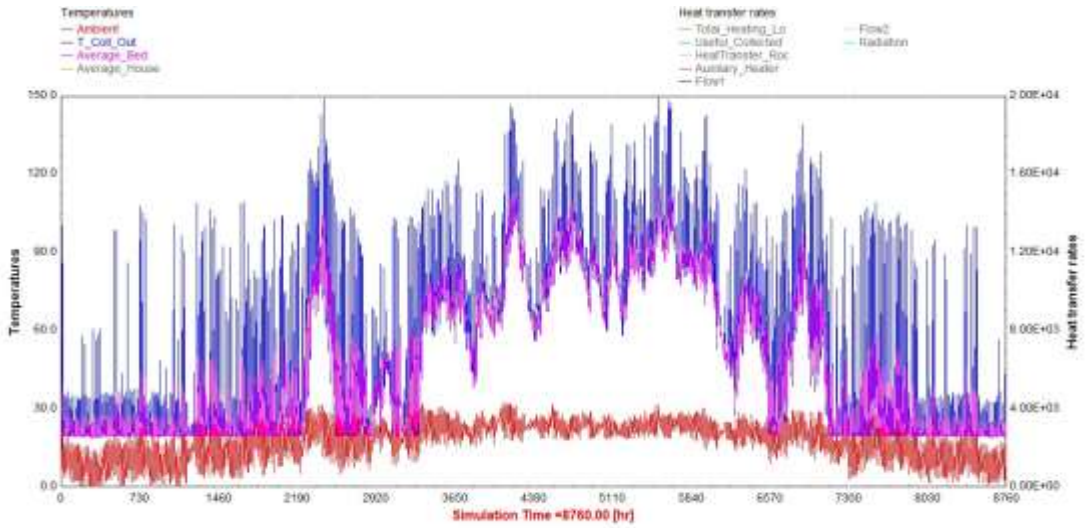

Figure 7.1 Temperature Plots for Yearly Simulation

The system model was simulated for the period of one year (8760 hours) at the time interval of 20 minutes. The temperature plots of different components are shown in the above Figure 7.1. The red profile is of the ambient temperature generated from the weather file whereas the blue lines depicts the collector outlet temperature which reaches more than 80 ℃ during the summer seasons. The pink depiction is of the average bed temperature which follows the increment and decreasing profile of the collector outlet temperature as it is charged during when the collector outlet temperature is high due to incident of solar radiation. The room temperature was kept constant at 20 ℃. The output of daily simulated results for area 4 m^2 and flow rate 0.0645 kg/s are presented in Appendix I.

Similarly Figure 7.2 represents heat transfer rates for the simulated period by solar air collector, pebble bed storage and auxiliary heater when it is required. During heating months namely October, November, December, January, February and March, the pink depiction represents the energy supplied by the pebble bed while the magenta is useful energy collected by the solar air collectors. The brown line represents the rate of energy supplied by the auxiliary heater to maintain the room temperature whenever its operation is required.

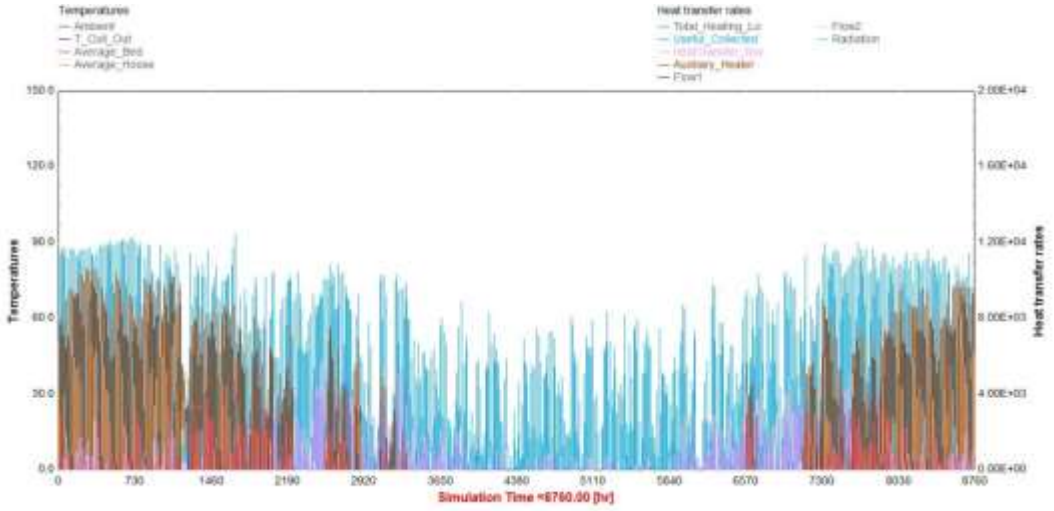

Figure 7.2 Heat Transfer Rates from Different Components

To study the nature of temperature distribution during day and night time the simulation was run from 6024 to 6096 hrs. which corresponds to September 6-8 of simulation time.

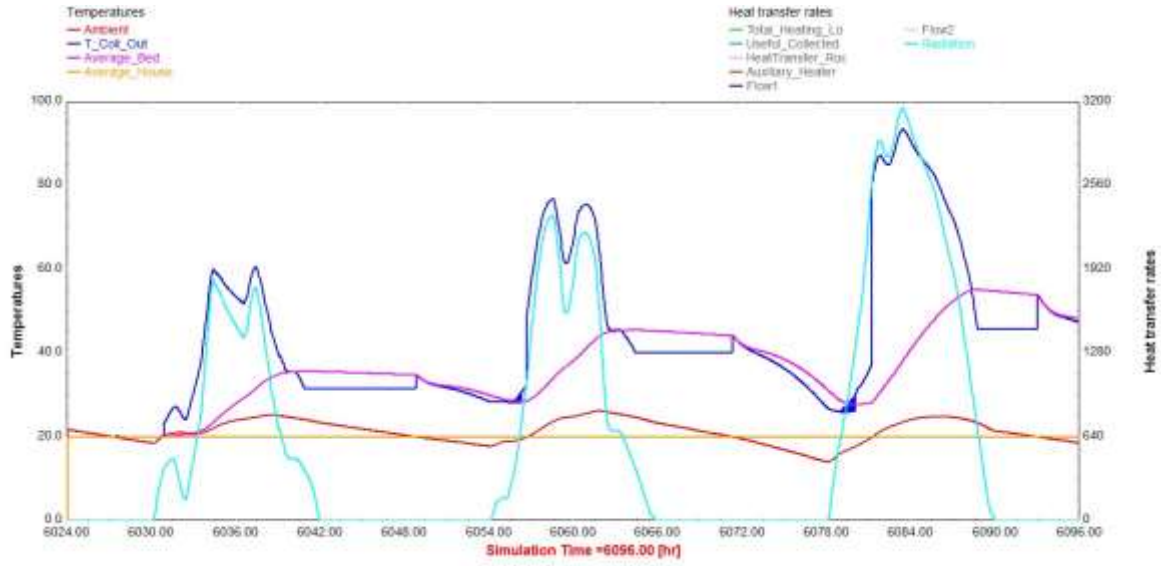

Figure 7.3 Temperature Profiles of Pebble Bed

Figure 7.3 shows average temperature of the pebble bed, collector outlet temperature, ambient temperature, average room temperature, and solar radiation for 6024 to 6096 hours, corresponding to the test days on September six through eight. It is seen that the average temperature of the pebble bed rises during the sunshine hours when the collector outlet temperature is also high as depicted by blue line and reaches around 30 degrees as depicted by pink line. When the ambient temperature gets lower than 20

degrees which eventually reduces the room temperature then the energy from the pebble bed is utilized due to which the average temperature of the bed decreases during utilization of energy.

Table 7.1 represents the thermal performance data of the system of multiple simulations run under different parametric conditions for the months October, November, December, January, February and March. First set of simulations were run by setting the flow rate to 0.0645 kg/s in the collector loop to utilize the performance data obtained during the experimental tests with same flow rate. Then same system was simulated with increasing the collector area from 2 m^2 to 4 m^2. And while the other parameters were kept constant, the flow rate was changed to 0.344 kg/s and the respective collector parameter $F_R(\tau\alpha)\ and\ F_R U_L$ were changed. And to study the effect of change in collector area, the collector area was increased to 4 m^2.

Table 7.1 Thermal Performance Data

		Flowrate at Collector loop=0.0645 kg/s						Flowrate at Collector loop=0.0344 kg/s					
		Heating Months						Heating Months					
Parameters	Area	Oct	Nov	Dec	Jan	Feb	Mar	Oct	Nov	Dec	Jan	Feb	Mar
Total Solar Radiation(MJ)	2	1290.81	1577.89	1446.14	1651.56	1291.54	1317.47	1290.81	1577.89	1446.14	1651.56	1291.54	1317.47
	4	2581.62	3155.80	2892.28	3303.12	2583.07	2634.94	2581.62	3155.80	2892.28	3303.12	2583.07	2634.94
Useful Energy Collected (MJ)	2	824.70	1061.43	955.76	1084.47	836.01	878.96	536.60	691.31	577.52	659.27	518.47	556.41
	4	1481.00	2093.27	1949.50	2244.15	1699.79	1701.24	939.82	1291.48	1186.87	1370.20	1034.63	1042.14
Collector Efficiency	2	0.64	0.67	0.66	0.66	0.65	0.67	0.42	0.44	0.40	0.40	0.40	0.42
	4	0.57	0.66	0.67	0.68	0.66	0.65	0.36	0.41	0.41	0.41	0.40	0.40
Total Heating Load (MJ)	2	929.82	2220.05	3576.78	4035.92	2929.95	2036.91	929.82	2220.05	3576.78	4035.92	2929.95	2036.91
	4												
Pebble Bed Contribution (MJ)	2	356.48	321.60	264.31	311.53	265.66	284.89	245.36	214.22	140.30	170.24	152.10	196.70
	4	552.33	600.31	465.58	569.80	440.96	518.70	382.00	369.29	302.51	360.96	294.14	326.05
Auxuliary Contribution (MJ)	2	573.34	1898.44	3312.48	3724.39	2664.28	1752.02	684.46	2005.83	3436.49	3865.68	2777.84	1840.21
	4	377.49	1619.73	3111.21	3466.12	2488.98	1518.21	547.82	1850.76	3274.27	3674.96	2635.81	1710.86
Solar Fraction	2	0.38	0.14	0.07	0.08	0.09	0.14	0.26	0.10	0.04	0.04	0.05	0.10
	4	0.59	0.27	0.13	0.14	0.15	0.25	0.41	0.17	0.08	0.09	0.10	0.16

The heating load of the house is maximum in the months of December and January reaching the maximum value up to 4035 MJ and gradually reduces in February, March etc. and reaches to minimum value of 930 MJ for the month of October. The pebble bed stores more energy when the collector area is increased from 2 m^2 to 4 m^2 and supplies maximum energy in January reaching 570 MJ. The proportion of energy supplied by auxiliary decreases by increasing the collector area and the maximum amount of energy supplied by the auxiliary is 3725 MJ for the month of January when the pebble bed is being heated by 2 m^2 collector area. The energy supplied by the auxiliary reduces to 3466 MJ in January by increasing the collector area to 4 m^2.

The proportion of energy supplied by the auxiliary increases and pebble bed decreases when the flow rate in the collector loop is reduced to 0.0344 kg/s as the heating load remains the same. The maximum energy supplied by the pebble bed is 382 MJ for the reduced flow rate corresponding to 4 m^2 of the collector area.

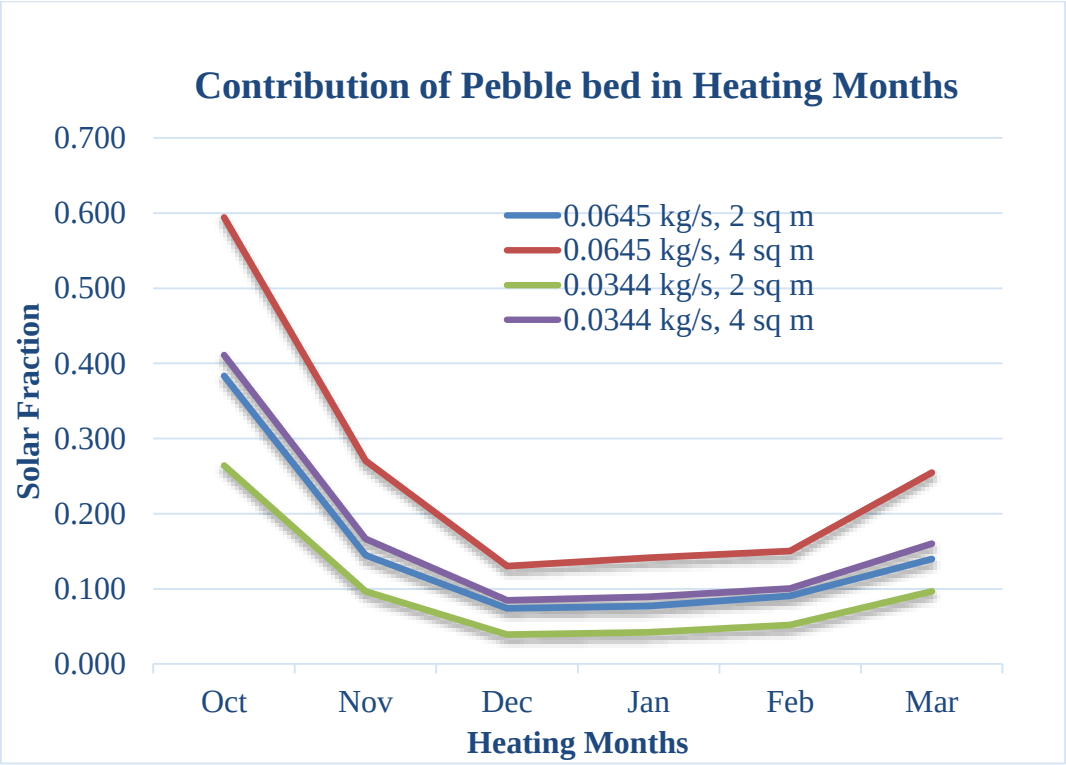

Figure 7.4 Solar Fraction for Different Heating Months

The solar fraction of the system is maximum for the month of October where the heating load is minimum. Gradually the proportion of solar fraction reduces for the month of October, November, December, January and slightly increases for the month

of February and March. Figure 7.4 depicts the variation of the Solar Fraction with heating months. It also shows the variation of the solar fraction in increasing and decreasing the collector area and flow rate in the collector.

Figure 7.5 shows the monthly heating performance of the proposed system for maximum flow rate of 0.0645 kg/s and maximum area of 4 m^2. It is maximum for the month of January and it clearly indicates the significant proportion carried out by Auxiliary Heater. The heating load also increases gradually from October up to January and then reduces.

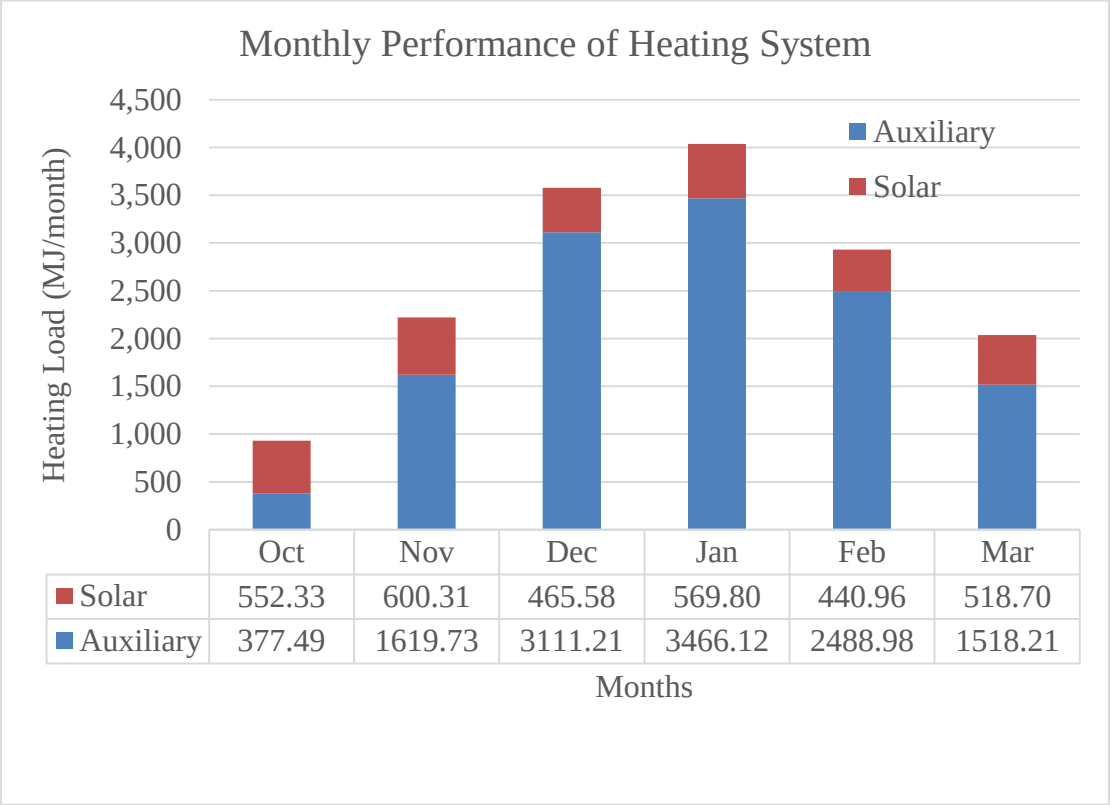

Figure 7.5 Monthly Heating Performance for maximum flowrate and area

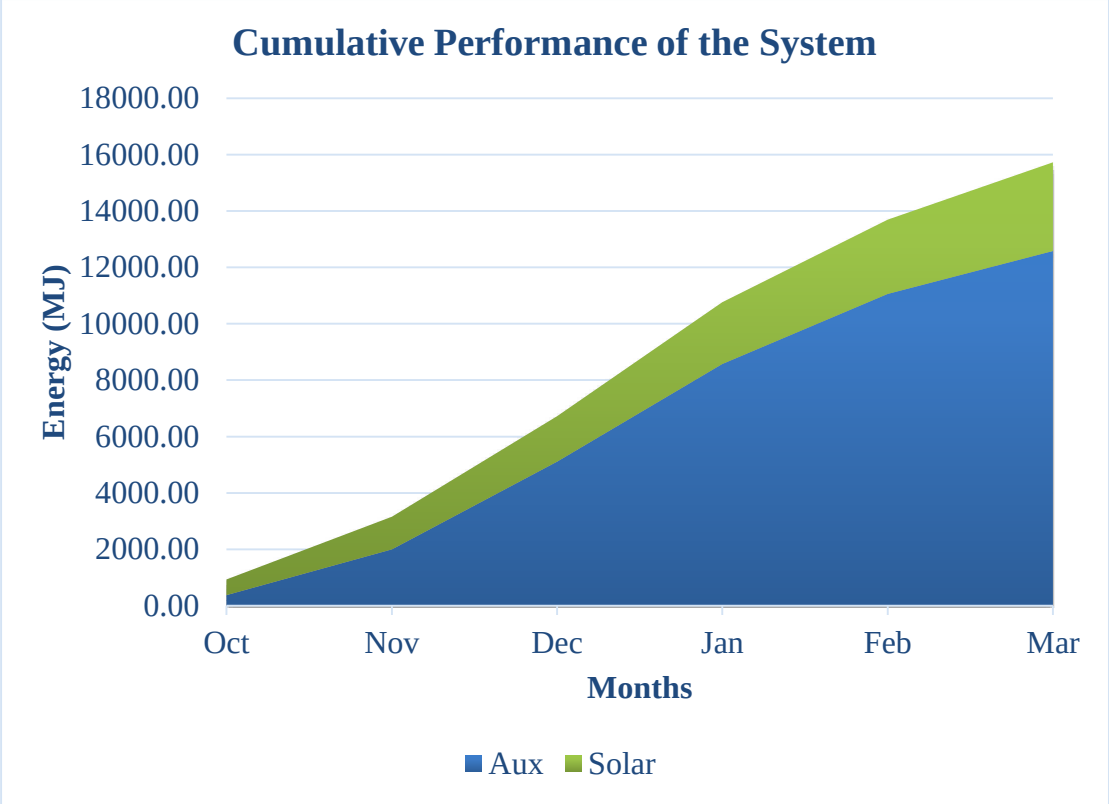

Figure 7.6 Cumulative Performance of the System

Figure 7.6 shows the cumulative performance plots for the heating season showing total loads (in MJ) and solar and auxiliary contribution to meeting the loads. The cumulative value for the total heating requirement, total energy supplied by the auxiliary and pebble bed is approximately equal to 15700 MJ, 12500 MJ and 3200 MJ respectively.

CHAPTER EIGHT

CONCLUSION AND RECOMMENDATIONS

8.1 Conclusions

The objective of the research was fulfilled and following conclusions are made:

- The system with Solar Air Collectors, manufactured in the country can be utilized to offset the energy cost associated with maintaining the space at desired set point temperature by supplying the energy form easily accessible solar source.
- The pebble bed system can supply on an average of 14% for the months December, January and February, around 26 % for March and November while reaching as high as 59 % for October of total heating load with 4 m^2 of collector area and flow rate of 0.0645 kg/s for the general living dwelling of floor area 150 sq. ft., typically prevalent for Kathmandu, for the heating months from October to March.

8.2 Scope for further work

The experiments with locally manufactured SAH and simulation using weather data of Kathmandu demonstrates that pebble bed thermal energy storage system can supplement the space heating load to the tune of 14% to 26 % depending on the month. In order to further this work it is recommended to:

- Install the proposed system and carry out the experimental verification of the additional components like pebble bed storage and load also.
- Assess the optimization of the components to arrive at the best mix of collector area, flow rate, and volume of pebble bed for different thermal load (spaces)
- Develop a pilot project for a small family single dwelling with complete financial analysis including first cost, operating cost and energy saving.
- The work can be further developed by incorporating evaporative cooler unit to utilize the same pebble bed as cooling unit during the need of the cooling. It further justifies the financial aspect of the project.

REFERENCES

Alam, T., Saini, R. & Saini, J., 2013. Heat and flow characteristics of air heater ducts provided with turbulators- A review. *Renewable and Sustainable Energy Reviews,* Issue 31, pp. 289-304.

ASHRAE, 2008. HVAC Systems and Equipments. In: s.l.:s.n.

Bekele, A., Mishra, M. & Dutta, S., 2014. Performance Characteristics of solar air heater with surface mounted obstacles. *Energy Conversion and Management,* Issue 85, pp. 603-611.

Benli, H., 2012. Exprimentally derived efficiency and exergy analysis of a new solar air heater having different surface shapes. *Renewable Energy,* Issue 50, pp. 58-67.

Bhusan, B. & Singh, R., 2012. Thermal and thermohydraulic performance of roughened solar air heater having proturded absorber plate. *Solar Energy,* Issue 86, pp. 3388-3396.

Bindra, H., Bueno, P., Morris, J. F. & Shinnar, R., 2013. Thermal Analysis and exergy evaluation of packed bed thermal storage system. *Applied Thermal Engineering,* Issue 52, pp. 255-263.

Chamoli, S., Chauhan, R., Thakur, N. & Saini, J., 2012. A review of the performance of double pass solar air heater. *Renewable and Sustainable Energy Reviews,* Issue 16, pp. 481-492.

Choudhury, C., Chauhan, P. & Garg, H., 1995. Economic Design of a Rock Bed Storage Device for Storing Solar Thermal Energy. *Solar Energy,* 55(I), pp. 29-37.

Duffie, J. A. & Beckman, W. A., 2013. Solar Engineering of Thermal Processes. In: s.l.:John Wiley & Sons.

Hernandez, A. L. & Quinez, J. E., 2013. Analytical models of thermal performance of solar air heaters of double-parallel flow and double-pass counter flow. *Renewable Energy,* Issue 55, pp. 380-391.

Ho, C.-D., Yeh, H.-M. & Chen, T.-C., 2011. Collector efficiency of upward-type double-pass solar air heaters with fins attached. *International Communications in Heat and Mass Transfer,* Issue 38, pp. 49-56.

Kalogirou, S., 2006. Solar Energy Engineering: Processes and Systems. In: s.l.:Elsevier.

Karaki, S., Duff, W. & Lof, G. O. G., 1978. *A Performance Comparision Between Air and Liquid Residential Solar Heating Systems*, s.l.: Solar Energy Applications Laboratory - Colorado State University.

Kurtbas, I. & Durmus, A., 2004. Efficiency and exergy analysis of a new solar air heater. *Renewable Energy*, Issue 29, pp. 1489-1501.

Melo, M. & Persson, T., 2013. *Economic Evaluation of Solar Charged Thermal Energy Store for Space Heating*, s.l.: European Solar Engineering School .

Nowzari, R., Mirzaei, N. & Aldabbagh, L., 2015. Finding the best configuration of a solar air heater by design and analysis of experiment. *Energy Conversion and Management*, Issue 100, pp. 131-137.

Ozgen, F., Esen, M. & Esen, H., 2009. Experimental investigation of thermal performance of a double-flow solar air heater having aluminium cans. *Renewable Energy*, Issue 34, pp. 2391-2398.

Raghav, G. & Nagpal, M., 2015. Performance Investigation and Optimization of Low Temperature Sensible Heat Solar Energy Storage System. *International Journal of Renewable Energy Research*, 5(3).

Romdhane, B. S., 2007. The air solar collectors: Comparative study, introduction of baffles to favor the heat transfer. *Solar Energy*, Issue 81, pp. 139-149.

Saini, R. & Singal, S., 2007. A review on roughness geometry used in solar air heaters. *Solar Energy*, Issue 81, pp. 1340-1350.

Saxena, A. & Goel, V., 2013. Solar Air Heaters with Thermal Heat Storages. *Chinese Journal of Engineering.*

Saxena, A., Srivastava, G. & Tirth, V., 2015. Design and thermal performance evaluation of a novel solar air heater. *Renewable Energy*, Volume 77, pp. 501-511.

Saxena, A., Varun & El-Sebaii, 2015. A thermodynamic review of solar air heaters. *Renewable and Sustainable Energy Reviews*, Volume 43, pp. 863-890.

Singh, H., Saini, R. & Saini, J., 2010. A review on packed bed solar energy storage systems. *Renewable and Sustainable Energy Reviews*, Issue 14, pp. 1059-1069.

Singh, R., Saini, R. & Saini, J., 2009. Models for Predicting Thermal Performance of Packed Bed Energy Storage System for Solar Air Heaters- A Review. *The Open Fuels & Energy Storage Science Journal,* Issue 2, pp. 47-53.

V.S. Hans, R. S. J. S., 2010. Heat transfer and friction factor correlations for a solar air heater duct roughened artifically with multiple V-ribs. *Solar Energy,* Issue 84, pp. 898-911.

Wang, M. Y., 2014. Design and Optimisation of a solar air heater with offset strip fin absorber plate. *Applied Energy*, Issue 113, pp. 1349-1362.

Yongsiri, K., Eiamsa-ard, P., Wongcharee, K. & Eiamsa-ard, S., 2014. Augumented heat transfer in a turbulent channel flow with inclined detached-ribs. *Case Studies in Thermal Engineering,* Issue 3, pp. 1-10.

Zhao, D., Li, Y., Dai, Y. & Wang, R., 2011. Optimal study of a solar air heating system with pebble bed energy storage. *Energy Conservation and Management,* Volume 52, pp. 2392-2400.

APPENDICES

APPENDIX I (DAILY SIMULATED RESULTS)

APPENDIX II (TRNSYS REFERENCE)

APPENDIX III (LETTER OF CONSENT)

APPENDIX IV (BLOWER DATA SHEET)

AC Fan

φ172mm

San Ace 172

51mm thick (Sidecut type)
51mm thick (Round type)
51mm thick (Round type /with sensor)

Only standard fans (without sensors) have acquired CSA certification.

General Specifications

- Material ····· Frame: Aluminum,
  Impeller: Plastics (Flammability: UL94V-1)
- Expected Life ····· Refer to specifications (L10:Survival rate: 90% at 60℃ , rated voltage,and continuously run in a free air state)
- Dielectric Strength ····· 50/60Hz 1,500VAC 1minute (between input terminal and frame)
- Dielectric Strength (With Sensor)···· Between AC input and DC input(Sensor output)
  : 50/60Hz 1,000VAC 1minute
  Between AC input and G
  : 50/60Hz 1,500VAC 1minute,
  Between G and DC input(Sensor output)
  : 50/60Hz 1,000VAC 1minute
- Sensor-Purpose Lead Wire···· ⊕ brown ⊖ black (Sensor) yellow
- Storage Temperature ····· −30℃ to+70℃ (Non-condensing)
- Operating Voltage Range···· Voltage of each model ±10%

Airflow - Static Pressure Characteristics

Standard

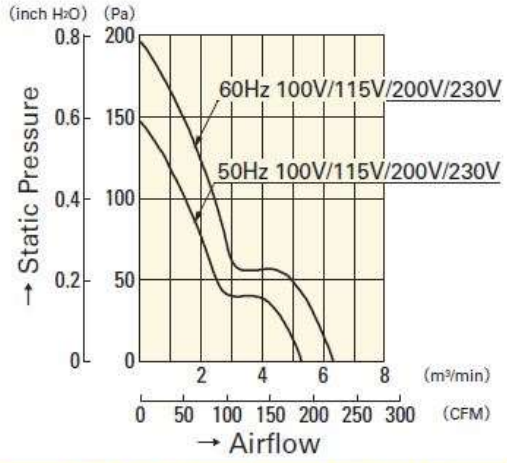

109-311	109-314
109-312	109-313

with Sensor

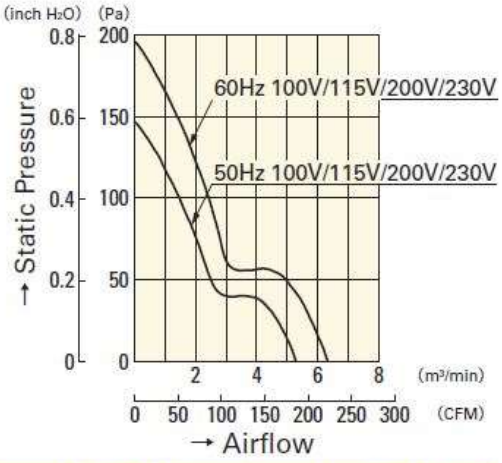

109-371	109-374
109-372	109-373

Characteristics of fan (Higher Flow Rate)

SUNON.

120x120x38 mm

70~117 CFM

■ Specifications

Model	P/N	Bearing	Rating Voltage	Freq.	Power Current	Power Consumption	Speed	Air Flow	Static Pressure	Noise	Weight
		● MVB ○ HBL ◎ Sleeve	(VAC)	(Hz)	(AMP)	(WATTS)	(RPM)	(CFM)	(Inch-H2O)	(dB(A))	(g)
DP200A	2123XSL.GN	◎	220-240	50/60	0.14/0.12	22/21	2700/3100	95/115	0.33/0.38	44/49	550
DP200A	2123XST.GN	◎	220-240	50/60	0.14/0.12	22/21	2700/3100	95/115	0.33/0.38	44/49	550

■ Air Flow-Static Pressure Characteristics

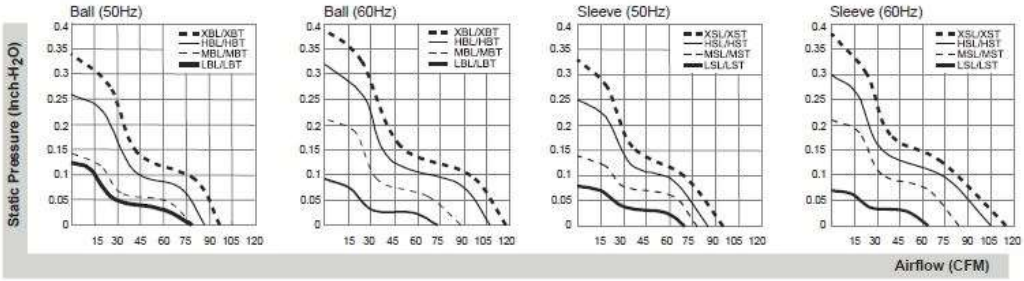

■ External dimensions(mm)

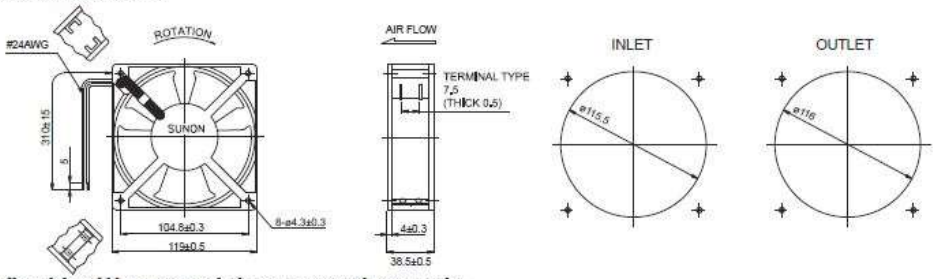

*All model could be customized. Please contact with Sunon Sales.
*Specifications are subject to change without notice. Please Visit SUNON website at http://www.sunon.com for update information.

Characteristics of fan (Lower Flow Rate)

APPENDIX V (USEFUL ENERGY COLLECTED)

APPENDIX VI (UNCERTAINTY ANALYSIS)

The result R is a given function in terms of the independent variables. Let w_R be the uncertainty in the result and w1, w2,., wn be the uncertainties in the independent variables. The result R is a given function of the independent variables x1, x2, x3,., xn. If the uncertainties in the independent variables are all given with same odds, then uncertainty in the result having these odds is calculated by

$$w_R = \left[\left(\frac{\partial R}{\partial x_1} w_1\right)^2 + \left(\frac{\partial R}{\partial x_2} w_2\right)^2 + \left(\frac{\partial R}{\partial x_3} w_3\right)^2\right]^{1/2}$$

The independent parameters measured in the experiments reported here are: collector inlet temperature, collector outlet temperature, ambient temperature, air velocity and solar radiation.

To carry out these experiments, mercury thermometers with an accuracy of 0.5 ℃ , anemometer(AR368) with accuracy ±3%, and pyranometer(Soldata 98 HP) with accuracy ±3% were used.

From the measured data, collector efficiency, mass flow rate and $(T_{a,out} - T_{a,in})/G_t$ were calculated. Equation of efficiency is:

$$\eta = \dot{m} C_p (T_{a,out} - T_{a,in})/(A_c G_t)$$

If Ac and Cp are considered constants, it can be written as

$$\eta = f(T_{a,out}, T_{a,in}, G_t, \dot{m})$$

Equation for mass flow rate

$$\dot{m} = \rho A_c v$$

Considering Ac and ρ be constant

$$\dot{m} = f(v)$$

Total uncertainty for mass flow rate can be written as

$$w_{\dot{m}} = \left[\left(\frac{\partial \dot{m}}{\partial v_a} w_{v_a}\right)^2\right]^{1/2}$$

Similarly , the total uncertainty for collector efficiency and $(T_{a,out} - T_{a,in})/G_t$ can be written as:

$$w_\eta = \left[\left(\frac{\partial \eta}{\partial \dot{m}} w_{\dot{m}}\right)^2 + \left(\frac{\partial \eta}{\partial T_{a,out}} w_{T_{a,out}}\right)^2 + \left(\frac{\partial \eta}{\partial T_{a,in}} w_{T_{a,in}}\right)^2 + \left(\frac{\partial \eta}{\partial G_t} w_{G_t}\right)^2\right]^{1/2}$$

$w_F = \left(\frac{\partial F}{\partial T_{a,out}} w_{T_{a,out}}\right)^2 + \left(\frac{\partial \eta}{\partial T_{amb}} w_{T_{amb}}\right)^2 + \left(\frac{\partial \eta}{\partial G_t} w_{G_t}\right)^2$ where

$F = \frac{T_{a,in} - T_{amb}}{G_t}$

The total uncertainty in determining flow rate, efficiency and $\frac{(T_{a,in} - T_{amb})}{G_t}$ are 3%, 8.2 % and 7 % respectively.

APPENDIX VII (EXPERIMENT PICTURES)

Test Setup

Blower Fitted in Duct

Measurement of Flow Rate

Manometer for measuring Pressure drop

Measurement of Solar Radiation